NASA CR-54087

TD/SSI-FR-21

EVALUATION OF CAPACITORS FOR SPACE PROPULSON APPLICATIONS

by

E. Blank, J. Freed, A. Winston

prepared for

NATIONAL AERONAUTICS AND SPACE ADMINISTRATION

CONTRACT NAS 3-2505

TOBE DEUTSCHMANN LABORATORIES

CANTON, MASSACHUSETTS

Request for copies of this report should be referred to

National Aeronautics and Space Administration
Office of Scientific and Technical Information
Attention: AFSS-A
Washington, D. C. 20546

NASA CR-~~54057~~ 54087
TD/SSI-FR-21

FINAL PROGRESS REPORT
EVALUATION OF CAPACITORS FOR SPACE PROPULSION APPLICATION

by

E. BLANK, J. PROUD, A. WINSTON

Prepared for:

NATIONAL AERONAUTICS AND SPACE ADMINISTRATION

CONTRACT NAS3-2505

Technical Management
NASA Lewis Research Center
Cleveland, Ohio
Project Manager
Peter Ramins

TOBE DEUTSCHMANN LABORATORIES
Canton, Massachusetts

ABSTRACT

32958

The development and evaluation of very low inductance energy storage capacitors, capable of long term performance at elevated temperature, is described. Based on general goals for capacitor characteristics in space propulsion applications, the central development problem is identified as the problem of attaining high temperature and high Q properties for materials employed in laminated capacitors. This need arises from the requirement to radiate self-generated heat while internal heating is reduced by employing low dissipation material. The report traces the development of fabrication techniques using a high temperature mica paper dielectric and describes the evaluation and testing of finished specimens. Dynamic testing is carried out at high repetition rates using a coaxial plasma gun as the electrical load, while the entire capacitor-gun system is operated in vacuum.

author

TABLE OF CONTENTS

TABLE OF FIGURES

TABLE OF TABLES

1. Introduction

In the development of repetitively pulsed plasma thrustors, an important, but for the present, weak link, is the energy storage system. The energy storage system must provide the necessary energy; it must provide high power; it must provide energy at high voltage to a load with time varying electrical characteristics; it must match the electrical characteristics of the load; it must withstand rapid discharging and charging; and it must withstand reversals in polarity. Beyond these requirements, the energy storage system for space application must have a long, useful lifetime; it must possess a high ratio of average power per unit weight; and it must be able to withstand the launch and space environment.

The present program was conducted to analyze and evaluate capacitor systems with the following design goals:

(1) Capacitances ranging from 1 to 100 microfarads
(2) Minimum self inductance, dissipation and weight
(3) Capacitor charging voltages ranging from 3 to 15 kilovolts
(4) Average power inputs up to 50 kilowatts at discharge repetition rates up to 1000 pps.
(5) Radiation cooled
(6) Useful lifetime of at least one year

Critical design parameters were to be determined as well as their interdependence. The Tobe Deutschmann Laboratories flat disc capacitor, Model ESC-247*, having low inductance and light weight, was to be used as a starting point. Based upon this, test model capacitors were to be designed, constructed and tested to meet the design goals. Capacitor testing was to be both static and dynamic in nature, the latter employing a repetitively pulsed plasma system.

The program was performed by the team of Tobe Deutschmann Laboratories and Space Sciences, Incorporated. The Tobe Deutschmann Laboratories, as prime contractor, was responsible for the design and fabrication of the test capacitors. Space Sciences, Incorporated, as subcontractor, was responsible for the evaluation of parameters and the determination of capacitor characteristics. Close cooperation and liason between the two groups was maintained

*Subject matter of pending U. S. and foreign patent applications, owned solely by Tobe Deutschmann Laboratories.

so that the evaluation of parameters and test results could be readily incorporated in improved capacitor design.

In the early part of the program, information was obtained from the majority of the manufacturers of energy storage capacitors to learn whether their designs or proposed approaches could meet or aid in meeting the design goal for plasma thrustors. No capacitor nor proposed design was uncovered by this search and consequently further attention was given only to the ESC-247 type. The existing ESC-247 design was for 0.5 joule capacitors. These were evaluated in static tests for determining material properties and for determining fabrication techniques employing new materials under investigation.

Based on the findings with these small units, larger units were constructed for dynamic testing, i.e., with a realistic plasma thrustor load. These larger units, designated ESC-247-C, were scaled-up versions of the ESC-247 to give ratings of 9 kilovolts and 0.31 microfarads for an energy content of 12.5 joules. These units were 24" in diameter by about 1/4" thick, less termination plates.

Considerable difficulty was encountered and finally overcome in developing ESC-247-C units that would not delaminate under test. Early in the program it was discovered that high temperature dielectric materials were necessary for proper performance. Several dielectric materials were investigated and on the basis of those investigated, Isomica (mica paper) was found to be superior in most regards. In constructing a high temperature capacitor, both the choice of dielectric and the method of bonding the dielectric sheets and foils are important. For example, the original ESC-247 units used Mylar as the dielectric. These units failed first in the adhesive holding the capacitor together and then from the inherent temperature limitations of the Mylar. With the Isomica units, mechanical failures were due only to the degradation of the bonding materials. In the latter half of the program this problem was overcome and units have been constructed and operated in dynamic tests with approximately 6 million discharges accumulated in the time available.

Dynamic testing has also been successfully carried out at reduced charging potentials with the plasma thrustor load operating up to 2000 pulses per second.

The results of a one year's program are presented in this report. The following section, Section 2, discusses the design and development of prototype test capacitors stemming from the basic ESC-247 design. Consideration is given both to the study of capacitor dielectric materials as well as to capacitor fabrication techniques. Sections 3 and 4 describe the tests performed on the test capacitors and the results of these tests. The details of the plasma thrustor load for dynamic testing of the capacitors are given. Both test methods and results are presented. Many of the tests have been designed specifically for this program and are not the conventional tests performed in usual capacitor rating. Section 5 draws together the pertinent findings. Included is a determination of the important parameters, the present degree of attainment of desirable properties, and the relationship of the capacitor to the thrustor.

2. Capacitor Development

2.1. Introduction

During the first month of the program, letters were sent to twenty-nine manufacturers who were listed in various directories as manufacturers of energy storage capacitors. The purpose of the letters was to determine whether any manufacturer had developed an energy storage capacitor that would approximate the design characteristics sought in this program. It was planned that if such capacitors could be found, they would be obtained for study and evaluation in the present program. The requirements placed on the capacitors and contained in the requests for information are listed in Table I.

Replies were received over a three-month period from seventeen of the solicited manufacturers. Of these responses, seven manufacturers stated that they did not manufacture energy-storage capacitors meeting the requirements nor did they immediately contemplate doing so. The remainder indicated some degree of willingness to consider the problem but did not presently supply capacitors approximating the specified characteristics. The majority of responses were based on conventional or standard capacitors designs as a basis for meeting the specifications. Consequently no capacitor nor a proposed design was uncovered by this search for inclusion in the program. Most replies indicated problem areas in attaining inductances in the nanohenry range, in providing for high temperature operation (above $40^{\circ}C$) and in achieving high discharge repetition rates up to 1000 pulses per second.

The Tobe flat-disc capacitor, Type ESC-247* designed and constructed prior to this program was selected for the start due to its low-inductance (approximately 1 nanohenry) and high Q (greater than 100). This capacitor and larger models, designated as ESC-247-C as developed, were the basic capacitors used during the course of the program. To meet the severe constraints imposed by the plasma thrustor application and the space environment, new materials had to be investigated for use in the manufacture of improved models. Very early in the program, it became

*Subject matter of pending U. S. and foreign patent applications, owned solely by Tobe Deutschmann Laboratories.

TABLE I

Capacitor Requirements

Capacitance: - 1-100 microfarads (in one or more units).

Internal Inductance: - Much less than .01 microhenry for individual units, somewhat less than .01 microhenry when more than one unit is employed to obtain the desired power as described below.

Operating Voltage: - 3 to 15 KV per single unit or for any series or parallel combination hereof.

Average Power: - Approaching 50 KW by operating units of highest energy content at a few pps or by operating low energy units at high repetition rate up to 1000 pps.

Operating Conditions: - Rapid discharge into low inductance load of approximately 0.1 microhenry or less. Capacitor will ring down with maximum voltage reversal of about 90%.

Thermal Stability: - Capacitor must be capable of high temperature operation at 100°C or more with radiational cooling only.

Duty and Life: - Repetition rates vary with energy content as described above. Capacitor life in continuous operation should be for at least one year.

Other Factors: - Weights of individual units or combinations should be minimal, while space requirements, although of secondary importance, should also be minimized. Any unusual geometry or termination configurations should be noted especially as they effect the arrangement of individual units in combination.

apparent that the capacitor must operate at very high temperatures and the program essentially consisted of developing capacitors utilizing the basic electrical design with materials that could operate in a severe environment for at least one year's service. The high temperature and vacuum environment put severe requirements on capacitor dielectrics and many possible materials were tested, evaluated and discarded as not being suitable. These materials are discussed in Section 2.3 of this report. The most promising material was Mica paper and it was this dielectric that received maximum attention during the course of this study. This material has been used by other capacitor manufacturers in the production of small capacitors but many problems had to be overcome to utilize it in the construction of capacitors of the size necessary to meet the program goals.

The following subsections of this section treat the electrical design of the energy-storage capacitor, the materials that were studied and the fabrication techniques employed.

2.2. Design Considerations

Capacitors that are to be used in conjunction with pulsed plasma thrustors must have many characteristics not found in conventional energy-storage capacitors. In addition to being light weight, long-lived and reliable, they must have low internal inductance and resistance compared to the inductance and resistance of the load. Most commercially-available, energy-storage capacitors are wound with Kraft paper and aluminum foil and impregnated with a liquid dielectric. Their design stress is often 2000 volts per mil and they are capable of operating for 10^3 to 10^5 discharges at a maximum teperature of $45^{\circ}C$ and at extremely low duty cycles. Their self-inductance is in the range of 15 to 150 nanohenries and the Q is typically 10 to 20 at the capacitor's self-resonant frequency. These commercially available capacitors must operate in a laboratory environment and cannot be subjected to extremes in either temperature, pressure or duty cycle.

The ESC-247 flat-disc capacitor possessed some of the desirable electrical properties required and was the basis for the development of capacitors during this program. The basic design has not changed but was rather scaled up to larger sizes and incorporated materials suitable for the service. The inductance of this type capacitor is less than 1 nanohenry and its Q greater than 100 at operating frequency. The physical construction is such that capacitors of this type can be electrically connected to coaxial systems without adding much series inductance and the high surface area to volume ratio is desirable for radiating capacitor power losses.

The ESC-247 is a disc-shaped capacitor having annular shaped terminals that are located on both faces of the capacitor as shown in Figure 1A. A through-hole in the center of the capacitor and concentric with the terminals permits efficient low inductance connections to coaxial circuits. The sizes constructed during this program range from 8" diameter x 1/8" thick to 24" diameter x 5/8" thick. The latter units store greater than 50 joules at stress levels of 1000 volts per mil.

The capacitor is constructed with twelve metallic plates stacked and separated by dielectric sheets. The capacitor plates are annular in shape having connecting tabs on the inner diameter as shown in Figure 1B. The dielectric sheets are processed with cutouts located to coincide with the inward projecting tabs of the capacitor plates. Two types of dielectric are used, one having five cutouts as shown in Figure 1C, and the other having six cutouts as shown in Figure 1D. The capacitor plates are stacked in pairs with the projecting tabs radially aligned and separated by dielectric sheets having five cutouts. The additional insulated pairs of plates are stacked with the tabs staggered in a spiral staircase fashion with dielectric sheets having six cutouts interposed between each pair of plates. The final stacked assembly is shown in Figure 1E. The capacitor is laminated under heat and pressure and, in its finished state, is uncased and self supported. The manufacturing process is described in Section 2.4.

The electrical parameters of a capacitor are quite often determined by the electrical properties of the dielectric. However, many capacitor

21-A1161

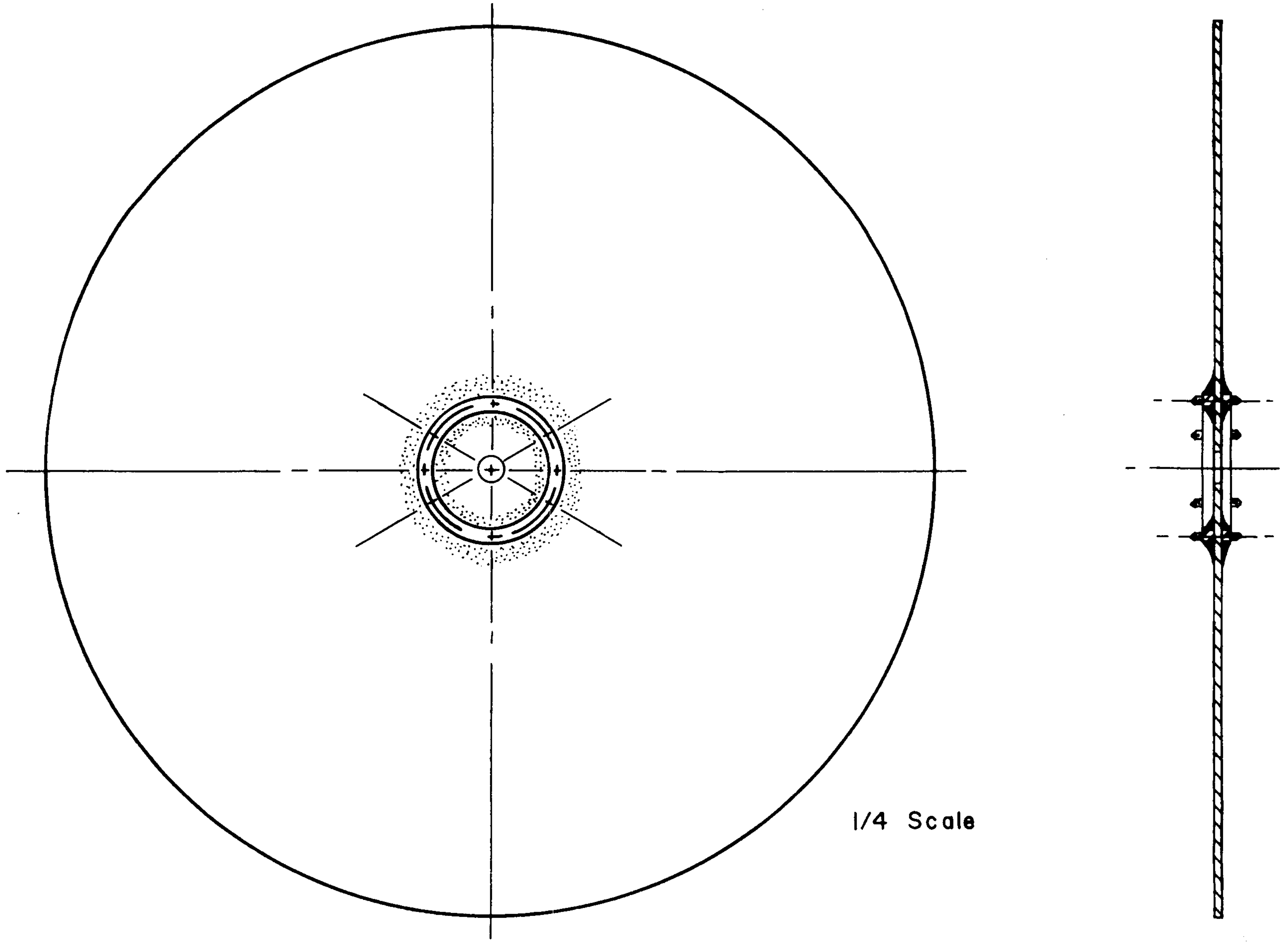

FIGURE IA. ESC247-C CAPACITOR

21-A2072

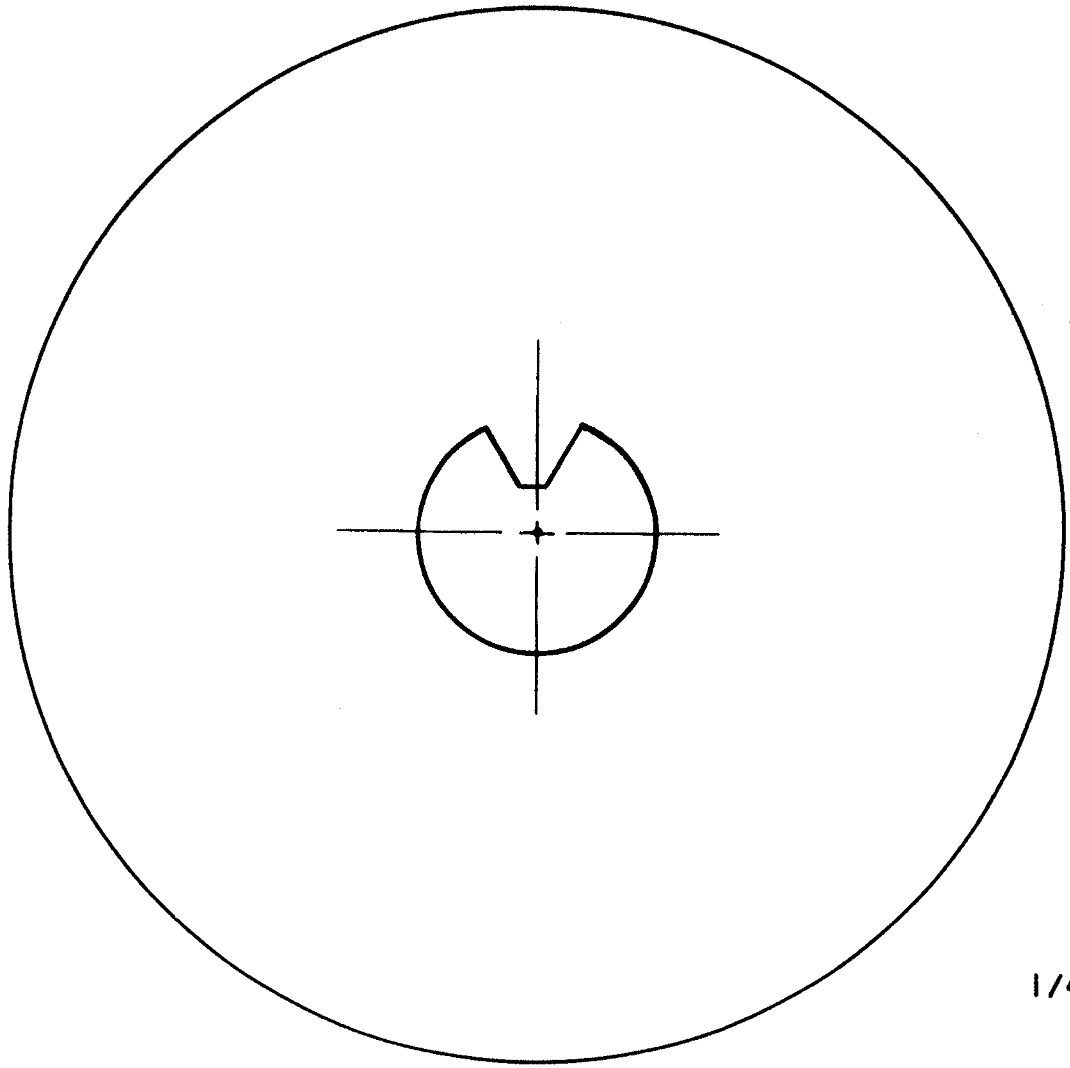

1/4 Scale

FIGURE IB. CAPACITOR PLATE

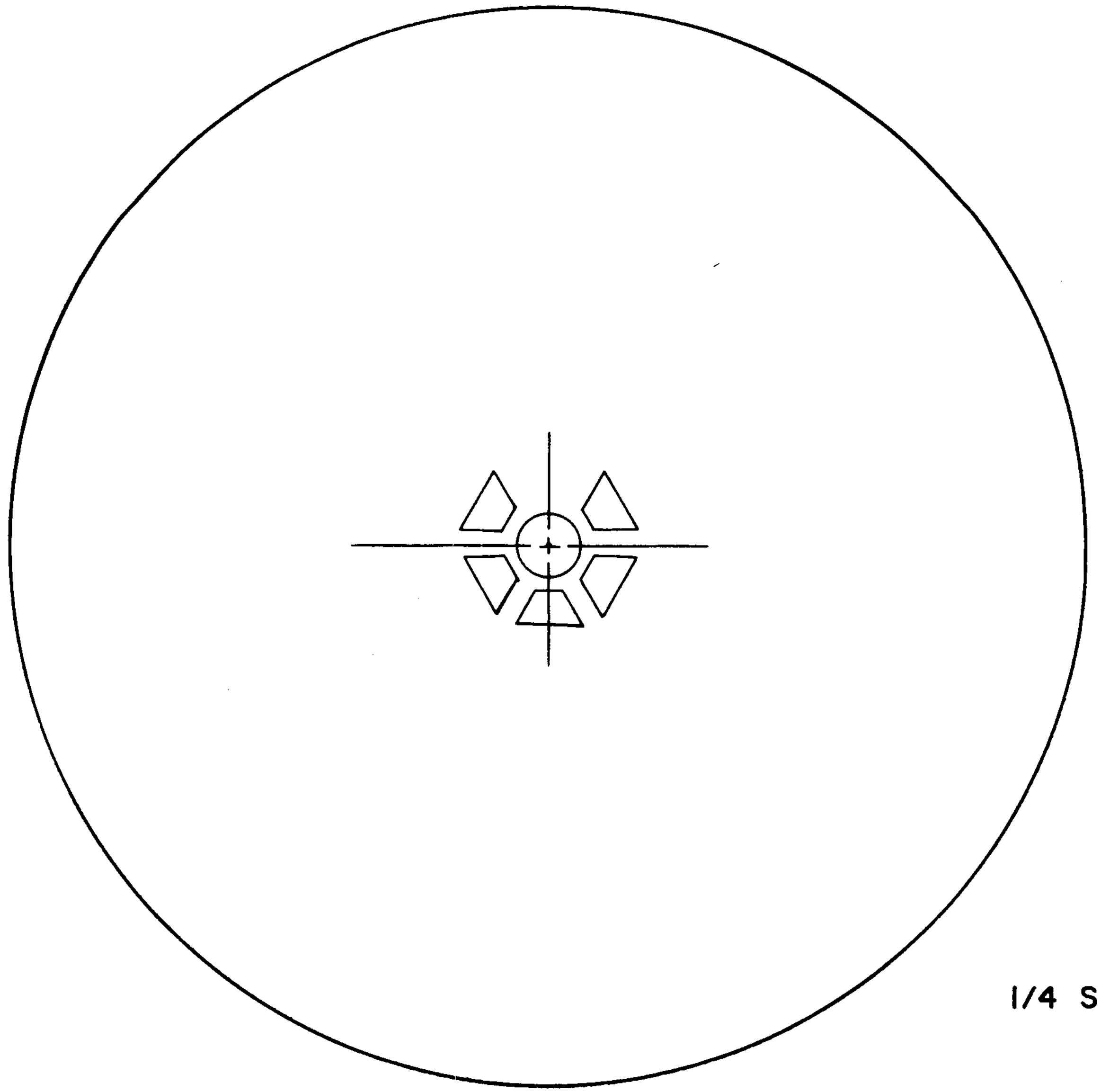

1/4 Scale

FIGURE IC. DIELECTRIC SHEET

21-A2073

21-A2074

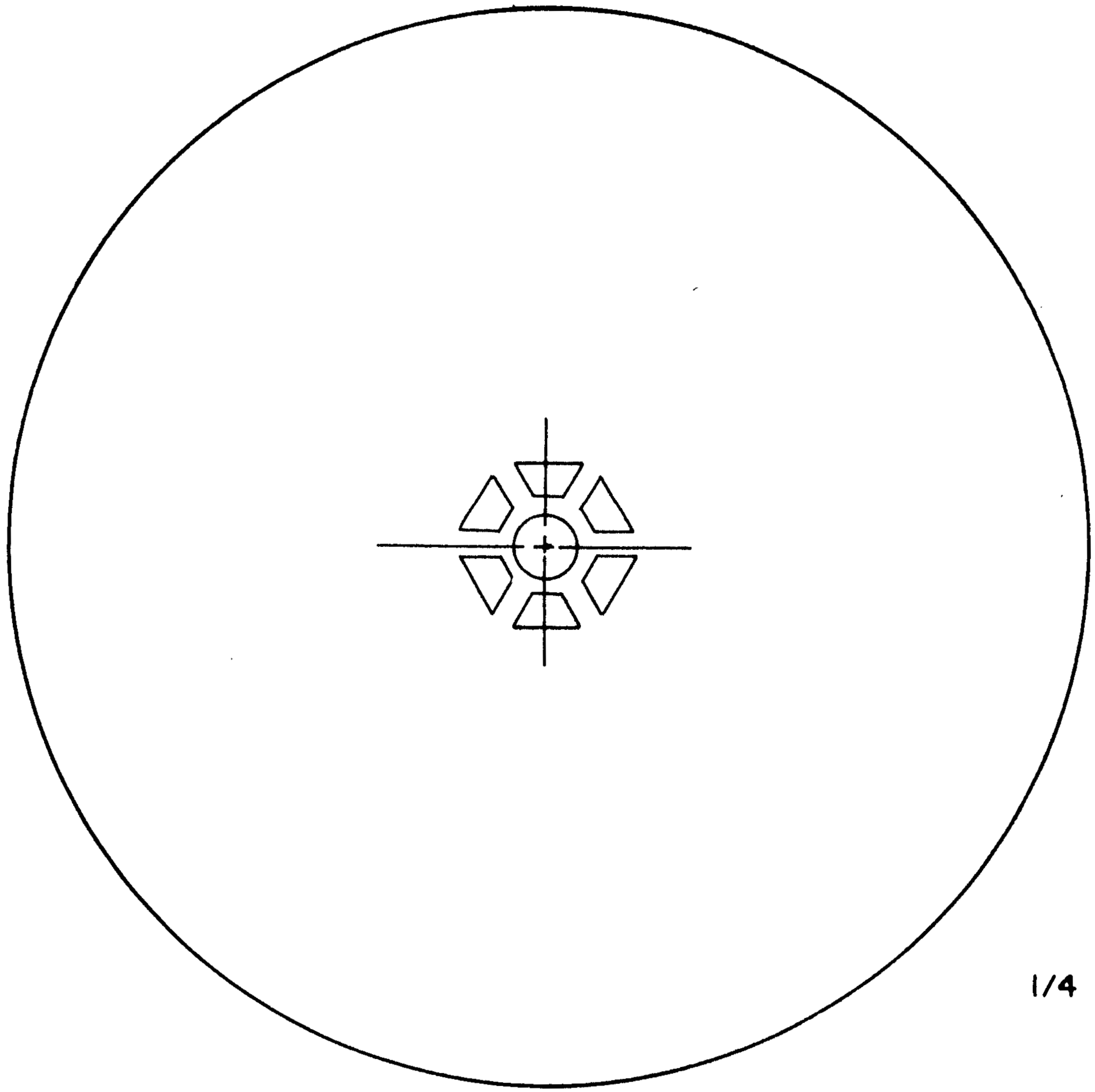

1/4 Scale

FIGURE ID. DIELECTRIC SHEET

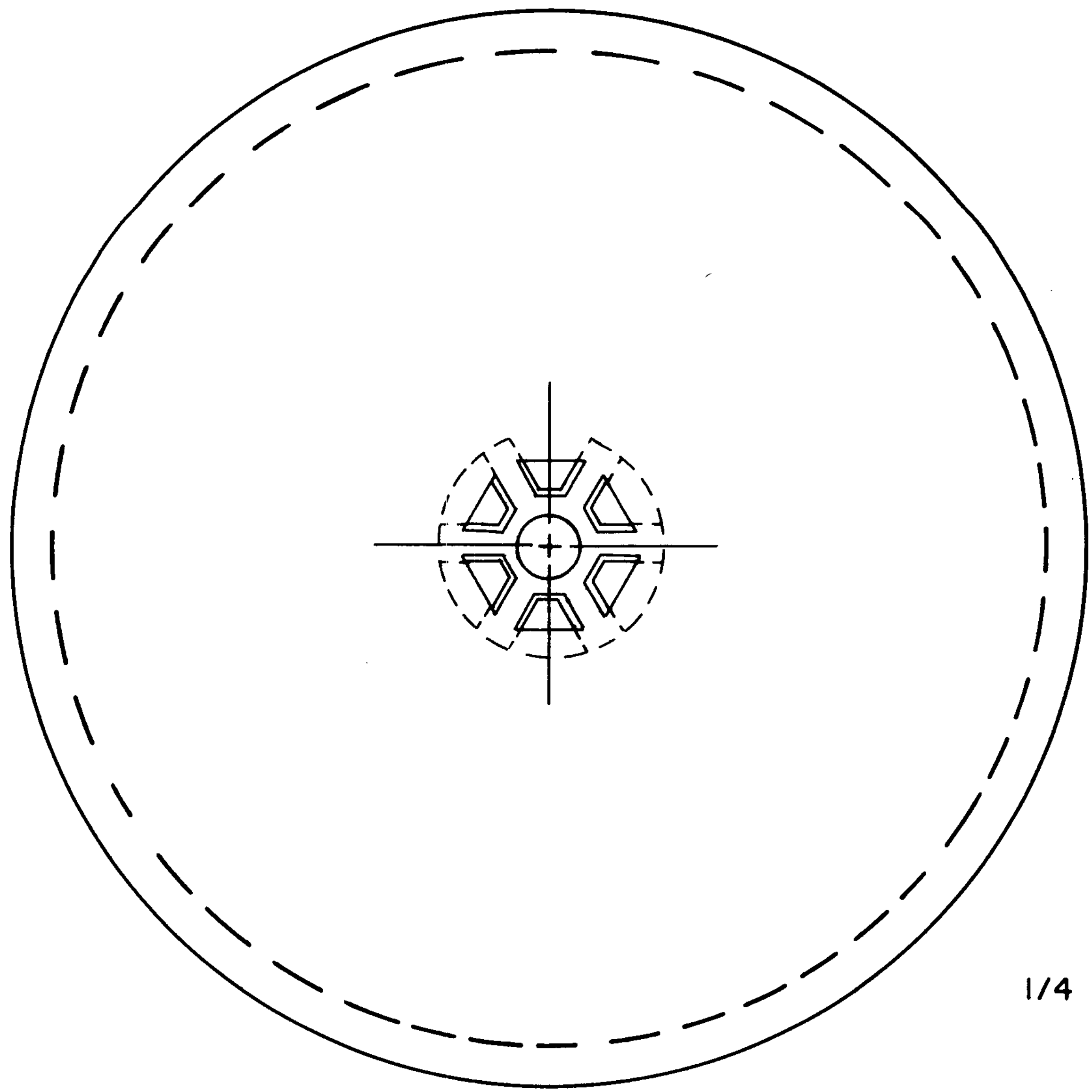

FIGURE IE. PLAN VIEW OF CAPACITOR ASSEMBLY designs that incorporate excellent dielectric material do not exhibit the high frequency properties of the dielectric, but rather are limited in performance by losses produced by the capacitor plates. The inductance and Q of energy-storage capacitors are often limited by capacitor plate geometry, size, construction and inter-connection.

To minimize capacitor losses, one must first use the proper dielectric and to prevent degradation of the dielectric properties, the capacitor plates must be of the proper thickness and geometry and be interconnected in the proper manner. The factors affecting the design of the ESC-247 type capacitor, including inductance, Q and dielectric strength, are described in this section.

To minimize the self inductance of a capacitor the currents during discharge should flow in opposite directions in adjacent conductors. For maximum field cancellation the current carrying members should be as close to one another as possible. In conventional energy-storage capacitors of the so-called low inductance, extended foil construction, the capacitor winding must be considered one conductor and the case the other. The inductance is calculated by considering the distance between the case and the average current sheath through the body of the winding. The physical volume necessary to house the capacitor necessarily makes this dimension large and is the limiting factor in obtaining low inductance. Rectangular bulk energy-storage capacitors utilize this principal and cylindrical "coaxial" capacitors are an improvement because they are would on hollow cores and more closely approach a low impedance coaxial cable.

The low inductance values characteristic of the flat-disc capacitor are realized because the magnetic field cancellation occurs internal to the capacitor. The current flow during discharge is in the opposite direction in adjacent foils and the separation between these conductors is on the order of .010 inch. Virtually all the inductance occurs at the termination and this value can be kept small (less than 1.0 nanohenry) by keeping the thickness of the capacitor to a minimum.

The Q of a capacitor is generally taken as the reciprocal of dissipation factor as measured on capacitance bridges at 60 or 1000 cps. Capacitors under 1.0 microfarads are measured at 1000 cycles and those over 1 microfarad are measured at 60 cycles. Typical oil impregnated capacitors have a dissipation factor of 0.5% and some plastic film units have a dissipation factor lower than 0.05%. These dissipation factors should correspond to Q of 200 and 2000, respectively. However dynamic measurements at self-resonant frequency consistently show Q of 10-20 in conventional wound capacitors irrespective of the dielectric. For example, conventional wound, energy-storage capacitors of the "non-inductive", extended-foil construction have been manufactured utilizing dielectrics with dissipation factors different by a factor of 100 to 1 over the frequency range of interest. When these capacitors are compared by bridge measurements at 1000 cycles, the 100 to 1 difference in dissipation factor is clearly indicated. Yet, when these same capacitors are tested for Q at their self-resonant frequency, the Q is approximately the same and lower than that expected in the dielectric.

Dielectric losses typically become worse as the frequency is increased. However, the dielectric losses do not approach the measured low Q figure. The low Q is attributed to foil losses.

Typical energy-storage capacitors use foil only .00025 inch thick and the conducting area is further reduced in use due to the strong magnetic fields that force discharge currents to the outer edges of the foils. The plates used in the capacitors evaluated in this program are .0043 inch thick and the shape and tabbing such that discharge currents are not impeded, and the Q realized very closely approaches that of the dielectric.

The dielectric strength of a capacitor is primarily determined by the dielectric properties of the material used in its construction. In addition, the geometry of the conducting plates, the spacing and size also have an important bearing. In high voltage capacitors one of the most important requirements is that the dielectric must be uniform and consistent throughout its entire thickness. Conducting particles inherent within the dielectric sheet are, of course, minimized during the manufacture of the basic material. Further safety is realized by using a multiplicity of layers thus reducing the possibility of conducting particles causing a premature failure. More important than this factor and possibly the major potential failure area is the presence of voids or inclusions of lower dielectric constant materials that can produce ionization and corona at high voltage stress. Corona of this nature generates severe localized heating and can very rapidly deteriorate some dielectrics that otherwise would be reliable and long-lived.

The dielectric used in the construction of ESC-247 capacitors can be produced void free by constructing to the methods described in Section 2.4. In addition, mica paper has the desirable property of not being degraded when operated in a corona atmosphere. No dielectric failures due to high voltage breakdown through the dielectric have occurred during this program and possible design changes to improve dielectric strength have not been incorporated.

The energy stored in a capacitor is obviously determined by the capacitance and the voltage to which the capacitor is charged. The limiting factor in charge voltage is the voltage stress of the dielectric which affects the capacitor's life. As mentioned earlier, common energy-storage capacitors may be stressed as high as 2000 volts per mil for low duty cycle operation. Other capacitors are designed at stresses of 1000 volts per mil and some even as low as 500 volts per mil, depending upon the duty, environment and life requirements.

Insufficient life test data have been gathered during the course of this program and the voltage stress was chosen at 1000 volts per mil as a starting point based on prior experience. The energy contents noted in this report may possibly indicate a rather large volume to energy stored ratio when compared to other capacitors. However, it must be realized that the ratings are assigned to capacitors based on this modest and conservative stress.

The insulation resistance of capacitors for plasma propulsion devices is not of paramount importance in their operation except as an indication of the quality of the capacitor. It is useful in gauging capacitors deterioration with use. Normally, the power loss, because of leakage current due to low insulation resistance, is a very small percentage of the total power applied to the capacitor and can be neglected. This problem may become significant in future work as higher temperatures are reached.

The insulation resistance of most dielectrics decreases rapidly with increase in temperature. The insulation resistance at the temperature ranges covered during the course of this program is sufficiently high (10^{10} - 10^{11} ohms) to disregard any power losses produced by this characteristics.

2.3. Materials

The materials used in the construction of flat-disc capacitors must be available in thin sheet form. The capacitor plates must have good electrical conductivity and both sheet copper and aluminum in thicknesses up to .005 inch were used. These readily available metals have proven quite satisfactory for the application and introduced no problems.

The dielectric must possess exceptional electrical properties over wide environmental ranges while maintaining the mechanical properties necessary for an unsupported and uncased laminated capacitor. Many plastic films, including Mylar, Teflon and H Film, have been evaluated during this program and found unsuitable for one or more reasons. Maximum effort was directed to the development of this type capacitor using Mica paper as the dielectric after initial testing indicated its advantage.

Mylar was the first dielectric evaluated in this program because successful manufacturing processes were established earlier. To construct Mylar film into stacked capacitors, an adhesive is required and many types were tested with fair success. E. I. Dupont type 4697-1 adhesive was found to be the best suited and was used exclusively in final test specimens. Standard roller coating techniques are quite satisfactory for applying the adhesive and produced satisfactory laminations.

The poor surface tracking properties of Mylar and the low service temperature (limited by adhesive), together with a dielectric constant and Q lower than Isomica, prompted discontinuance of this material in the program.

Teflon possesses a high dielectric strength and high temperature capabilities. However, Teflon's characteristic of not sticking to other materials defeats itself in its use as a laminated stacked capacitor. The high density of Teflon, coupled with its low dielectric constant, make the weight and size of capacitors prohibitive. The severe construction problems, cold flow characteristics, lack of good adhesive, low dielectric constant and weight eliminated Teflon early in the course of this program. ESC-247 capacitors were constructed with fair success. However, further work was discontinued.

H Film is a polyester material possessing properties quite similar to that of Mylar except over a greater temperature range. The limiting factor in constructing capacitors from H Film is the adhesive, and although the base material has properties better than Mylar, capacitors could not be constructed because of the limitations in the adhesives available. Therefore, other than making preliminary test samples, no other work was done on H Film.

The dielectric constant of Isomica (4.5 to 5) is approximately twice that of Teflon and approximately 50% greater than both Mylar and H Film. The short term dielectric strength of these materials is comparable (4000 V/mil). However, Isomica appears rather immune to corona while the other dielectric materials tested are adversely affected. These factors, together with Isomica's basically inorganic nature, prompted major effort in this type dielectric. In addition to Isomica, which is supplied pre-impregnated, unimpregnated mica paper was procured and impregnated with other commonly available silicone resins. The silicone resins tested were not equal to the pre-impregnated mica paper (Isomica) and further work was discontinued as the fabrication problems of Isomica were solved.

Initial testing of dielectrics involved the construction of 3-plate base capacitors measuring 6 x 6 inches. Basic fabrication procedures were experimentally determined and successful capacitors evaluated electrically. Promising materials passing both the electrical and mechanical requirements were constructed into ESC-247 capacitors of approximately 0.1 microfarads and manufacturing processes further improved.

2.4. Fabrication

The successful construction of 50-joule Isomica capacitors was preceded by many failures. After determining Isomica to be the material best suited, much had to be learned about manufacturing processes. Techniques learned constructing small sections would not scale for larger capacitors but required major revisions. The first laminations performed in the material study were based on the material manufacturer's recommendations. These techniques were based on their experience constructing 1 square inch capacitors and many test laminations were required before successful basic 3-plate capacitors were constructed. Fifty-four lamination cycles were necessary to construct successful 8" diameter ESC-247 capacitors and 15 lamination cycles required before successful 24" diameter ESC-247 capacitors were constructed.

The ESC-247-C capacitor is constructed utilizing seven sheets of .002 inch, precut Isomica between each conducting capacitor plate. The capacitor plates are constructed from .0043 inch copper sheet cut to shape. All sharp edges are buffed and polished to remove any possible burrs or slivers. The copper plates are then thoroughly washed in a solvent, such as MEK, to remove all oils and possible contaminants. A thin coating of GE type SR 224 silicone resin is applied to both surfaces of these plates and completely cured.

The capacitor stack is assembled as described in Section 2.2, utilizing the pre-processed component parts and is then subjected to a pre-heat cycle of sixteen hours at 105°C in an oven to remove all traces of absorbed moisture. The sixteen hours at 105°C should not be exceeded at this stage, in either time or temperature, as partial curing of the resin may result in a deterioration of the resin flow characteristics during final dure. The assembled unit is then subjected to a pressure of 100 microns for an additional 24 hours while maintaining heat to remove any additional traces of water vapor or solvent and is kept under vacuum with no heat until ready for final processing.

The prepared capacitor is sandwiched between stainless steel plates utilizing Teflon-coated, glass cloth as a slip sheet. This assembly is then inserted between aluminum carrier plates that have asbestos sheeting interposed to act as a thermal buffer and pressure compensation pad. This completed assembly is then inserted between the hydraulic press platens as shown in Figure 2.

Prior to the application of hydraulic pressure to the capacitor section, the platen assembly is evaluated to less than 100 microns to remove any air that may possibly become trapped during the pressing operation. A pressure of 500 pounds per square inch capacitor area is then applied to the system prior to the application of heat. The capacitor, evacuated and under compression, is now subjected to a linear temperature increase at the rate of 50^{o}C per hour until the first stage temperature of 175^{o}C is reached. It is at this point that the resin binder flows and, therefore, this temperature is maintained for approximately 2 hours. During this time, final pressure of 1000 pounds per square inch is applied. Vacuum pumping is continued to remove any volatile matter that may be liberated during the resin flow. Final curing temperature, (230^{o}C) is then applied for ten hours. The total curing time being reached, heat is shut off, full pressure is maintained, and a slow cooling cycle is begun until room temperature is reached. At this point the cycle is completed. The overall process flow sheet leading up to dynamic testing is illustrated in Figure 3.

The following table lists the manufacturing cycles of 24 inch diameter capacitors constructed with Isomica. The fabrication results as noted only indicate the relative progress obtained in fabrication as test results are indicated in Section 4. Capacitors commencing with cycle G were subjected to preliminary electrical tests including high potential testing prior to final evaluation.

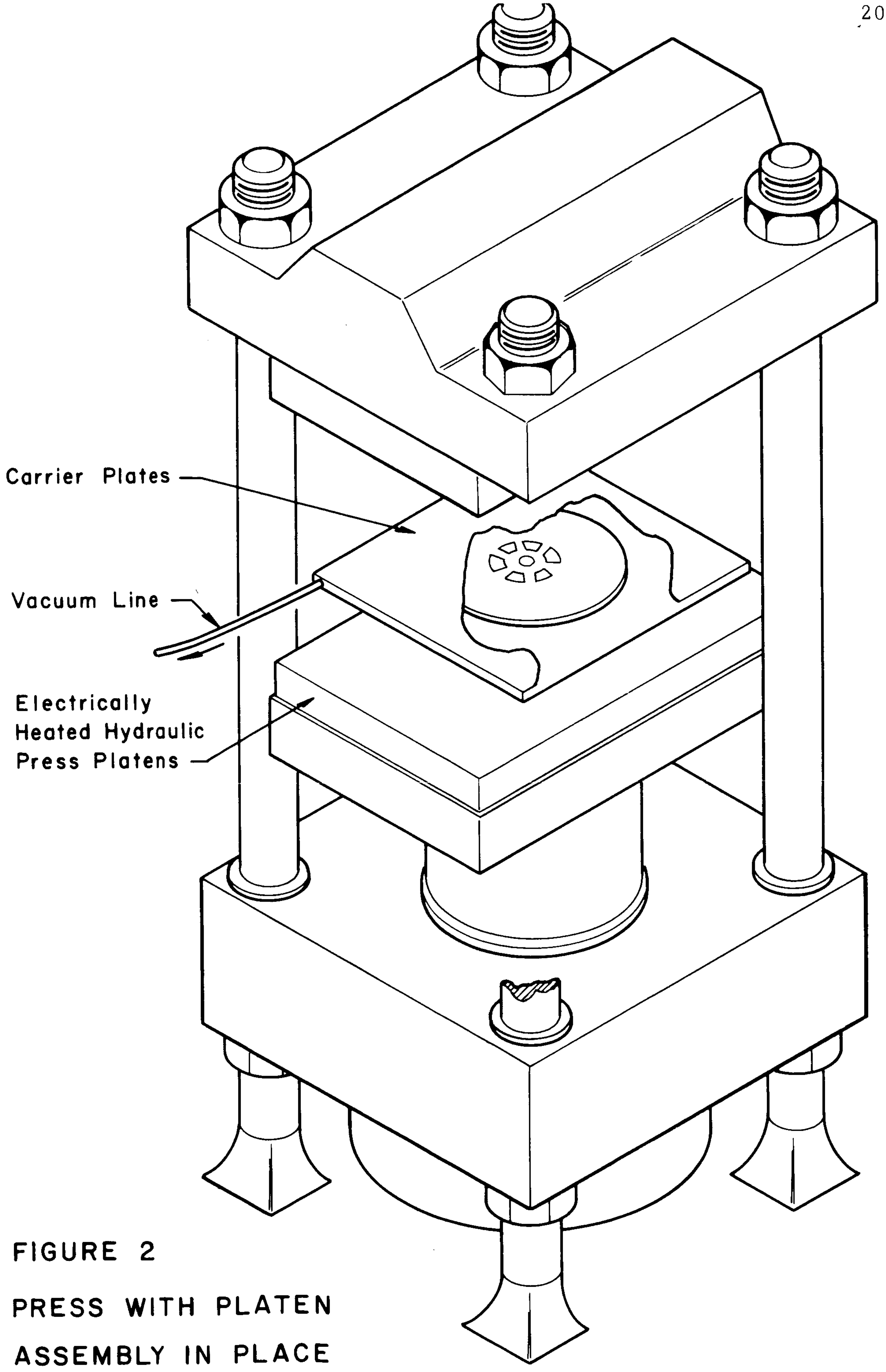

FIGURE 2

PRESS WITH PLATEN

ASSEMBLY IN PLACE

21-A2076

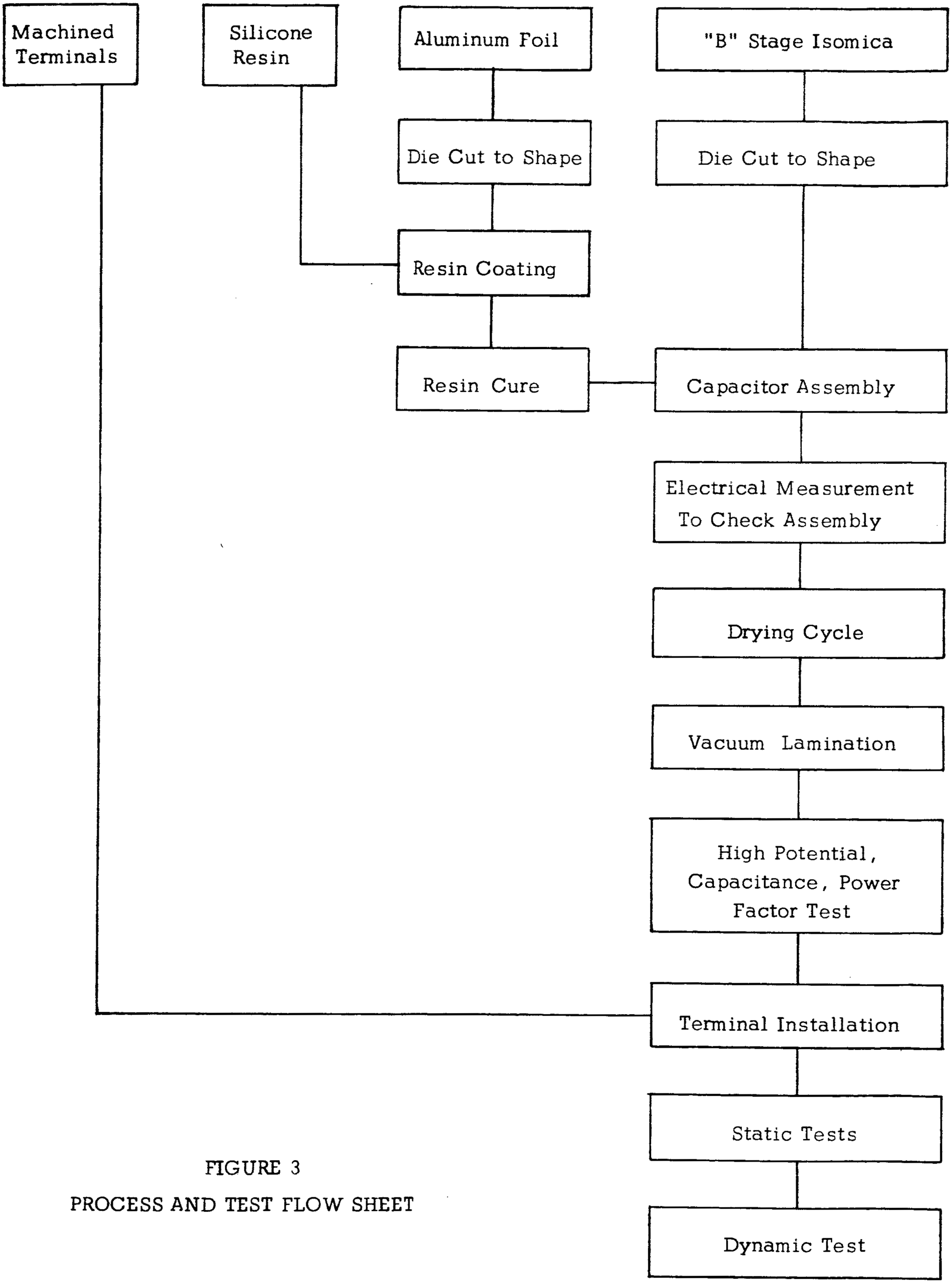

FIGURE 3

PROCESS AND TEST FLOW SHEET

TABLE II

Fabrication Cycles-24 Inch Isomica Capacitors

Identification Cycle	Capacitance (Microfarads)	Nominal Dielectric Thickness (mils)	Fabrication Results
A	Variable	14	Complete Delamination
B	Variable	14	Substantial Delamination
C	Variable	14	Partial Delamination
D	.195	14	Partial Delamination
E	.240	14	Partial Delamination
F	.228	14	Slight Delamination
G	.230	14	Slight Delamination
H	.235	14	Slight Delamination
I	.240	14	Partial Delamination Under Vacuum
J	.240	14	Partial Delamination Under Vacuum
K	.240	14	Partial Delamination Under Vacuum
L	.380	10	Slight Delamination Under Vacuum
M	.317	12	Excellent Lamination
N	.336	12	Excellent Lamination
O	.806	12	Excellent Lamination

3. Capacitor Evaluation (Static Testing)

3.1. Background, the Thermal Problem

The ESC-247 capacitor, developed prior to the program, has many of the characteristics which are of interest to space propulsion application. That is, it has a self-inductance of the order of one nanohenry, it has excellent power handling capability for its weight and it has a form factor (thin disc) which makes it well suited for radiational cooling of self generated heat. However, the low energy content (0.5 joules for high repetition rate duty) of this capacitor made clear at the outset that a scaled-up version would be necessary to approach the design goals of the program. Furthermore, it soon became apparent that new capacitor dielectric materials would be required for the high temperature capability inherent in these goals.

Capacitor evaluation in the early phases of the program was confined to measurements of the properties of the small ESC-247 unit. Emphasis was placed on investigating the basic electrical properties of the test units with special regard to variations with operating temperature. Testing was carried out with both standard and modified Mylar ESC-247 units and with first trial units employing Isomica as the dielectric material. The translation of the basic design to the ESC-247-C unit employing Isomica marked the close of static evaluation and initiation of dynamic tests under simulated operating conditions.

An analysis of heat generation within capacitor storage systems and within the load was carried out early in the program. The important conclusion was reached that the goals: (1) high repetition rate operation, (2) high average power and (3) radiational cooling require the use of capacitor materials with high temperature capability far beyond that of conventional capacitors. This conclusion led to program emphasis on the development and evaluation of capacitors employing low dissipation-high temperature dielectric materials. Therefore, the recognition of the thermal problem has influenced both the static and dynamic testing and evaluation phases of the program. The following analysis is presented to illustrate the problem quantitatively.

The analysis is carried out with respect to a simulated load in the form of a coaxial plasma gun. An evaluation of the partition of energy during operation of the simulated plasma propulsion load has been performed. In order to obviate a full analysis of the energy partition including an examination of the propulsion efficiency, an approach is taken whereby the significant sources of energy loss are singled out and labeled by an effective series circuit resistance as follows:

R_1 = effective series resistance of the capacitor

R_2 = actual series AC resistance of the discharge circuit

R_3 = effective series resistance of plasma to label all plasma energy which is transferred as thermal energy to the gun electrodes

R_4 = effective series resistance of plasma to label all plasma energy (internal, radiative and kinetic) which is expelled from the system

In a later section experiments are described in which an efficiency parameter η was measured where η is defined by

$$\eta = \frac{R_4}{R_1 + R_2 + R_3 + R_4} \tag{1}$$

Typical measured values under simulated operating conditions are approximately 0.25 indicating that 75% of the input electrical power appears as heat in the gun-capacitor system. A large fraction of this thermal power is generated within the load (i.e. in R_2 and R_3). In the absence of provision for cooling, the heat generated in the load is conducted to the capacitor which is then penalized by the need to radiate all system dissipated electrical energy. While this problem is quite general to capacitor-gun systems of the type simulated in this investigation, the thermal problem also exists with respect to the heat balance for losses within the capacitor itself.

Making use of the above definitions, an approximate analysis of the heat generation problem can be carried out using conventional circuit parameters. The overall circuit quality is then defined by:

$$Q = \left[\omega C \left(R_1 + R_2 + R_3 + R_4\right)\right]^{-1} \tag{2}$$

while the circuit quality of the capacitor under lossless load conditions is:

$$Q_1 = (\omega CR)^{-1} \tag{3}$$

The approximate circuit waveform is given by:

$$I = I_o \cdot \sin \omega t \cdot \exp\left(-\omega t/2Q\right) \tag{4}$$

Then, the energy expended in R_1, R_2, R_3 and R_4 during ring-down for N complete cycles is:

$$\begin{aligned} E &= \int_o^{t=2\pi N/\omega} (Q\omega C)^{-1} I_o^{\,2} \sin^2 \omega t \cdot \exp\left(-\omega t/Q\right) \cdot dt \\ &= E_o \left[1 - \exp\left(-2\pi N/Q\right)\right] \end{aligned} \tag{5}$$

where E_o is the initial stored energy.

The quantity, $\exp(-2\pi N/Q)$, represents the fraction of the initial energy remaining in the capacitor at the end of the discharge. Thus, so long as N/Q is not small compared with unity, the stored energy is fully dissipated during the discharge.

The total heat generated per discharge within the capacitor can then be expressed by:

$$H = \frac{Q}{Q_1} E_o \left[1 - \exp\left(-2\pi N/Q\right)\right] \doteq \frac{Q}{Q_1} E_o \tag{6}$$

Accurate evaluation of the heat generation then depends upon knowledge of Q and Q_1 at the desired operating frequency. Typical values for Q in plasma discharge devices of the type of interest here are of the order of 10, while Q_1 depends sensitively on the dielectric material employed in the storage capacitors. Measurements show that Q_1 in parallel plate Mylar capacitors is approximately 50, while materials such as Isomica exhibit qualities exceeding 100. Taking the typical value Q = 10 with Q_1 in the range 50 to 200, it is seen that the energy dissipated within the capacitor is between 5% and 20% of the stored energy per discharge.

The impact of this conclusion may be illustrated by application to a capacitor unit such as the ESC-247-C tested under this program. The unit parameters of importance to this discussion are its nominal energy content, 12.5 joules, and its effective radiating surface area, 5600 cm^2.

In order to estimate the equilibrium temperature rise in the test capacitors, the power loss by radiation has been equated to the rate at which heat is generated in the system. Most dielectric materials such as those encasing the test capacitors, have total thermal emissivities very near unity. Therefore, the total power radiated by the capacitor is given approximately by:

$$\sigma T^4 \cdot \text{area} \tag{7}$$

where $\sigma \doteq 5.7 \times 10^{-12}$ watts/cm^2 $(^\circ K)^4$ and T is the absolute temperature in $^\circ$K. Assuming that the capacitor "sees" a uniform absorbing ambient at scme lower temperature T_o, the net power loss is given by:

$$P_{net} = \sigma (T^4 - T_o^4) \cdot \text{area} \tag{8}$$

The value of T_o is not important in the estimate of P_{net} so long as T is significantly greater than T_o. For the present estimate of temperature rise T_o is taken to be room temperature ($T_o = 295^\circ K$).

Using equation (6) with the cited typical values of Q and Q_1 the self-generated heat per cycle is 0.63 to 2.50 joules/cycle. In thermal equilibrium, the thermal power radiated will be in the range 0.63 F to 2.50 F (watts) where F is the discharge repetition rate (pps). The equilibrium temperature rise is then determined from equation (8). The results are shown graphically in Figure 4. in which the operating temperature is plotted versus pulse repetition rate. It is emphasized that the results

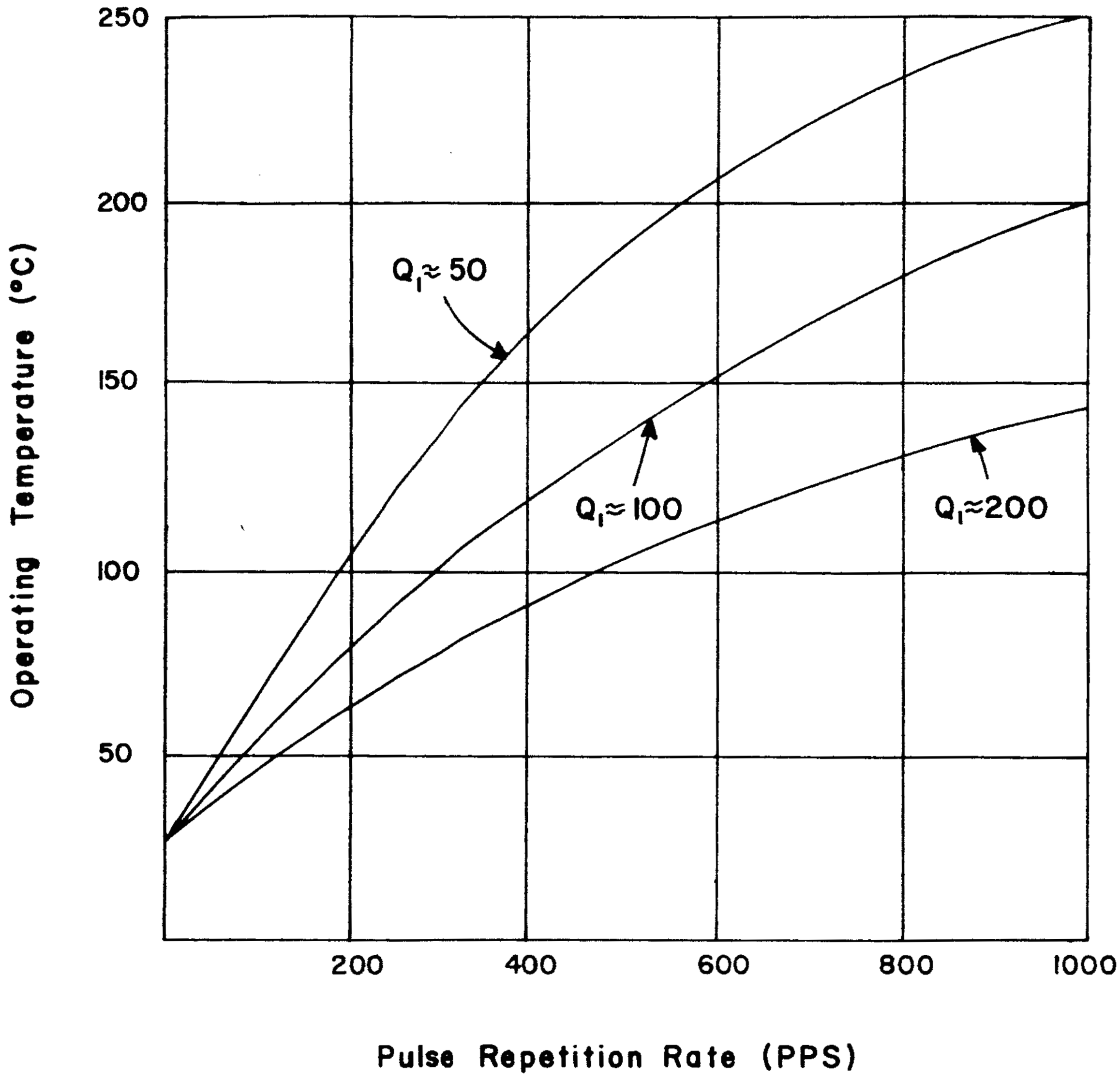

FIGURE 4

TEMPERATURE RISE OF ESC-247-C CAPACITOR FOR VARIOUS PULSE REPETITION RATES DUE TO SELF-GENERATED HEAT.

21A-A1401

shown are for self-generated heat only and that actual systems application may impose additional thermal loading. While these estimates are specifically for the ESC-247-C capacitor, this unit has an excellent form factor for radiating thermal power.

For these two reasons, the results are quite conservative in that substantially higher temperature operation might result in actual practice.

The results shown in Figure 4 demonstrate that Mylar, because of its relatively low Q and low maximum temperature capability (e.g. $\approx 100^{\circ}C$), is unsuited as a dielectric material for high average power applications. The need is clear for a capacitor capable of operating substantially above $100^{\circ}C$ with a high value for Q.

3.2. Quality Assurance Tests - Thermal Stability

All capacitors which were prepared for static tests and evaluation were first routinely examined in standard quality assurance tests. The purpose of such tests was to obtain a prompt initial appraisal of fabrication success prior to the more extensive evaluation which followed. These tests included a static high potential test of each unit at 150% of its rated voltage, a determination of room temperature capacitance and dissipation factor at 1000 cps and a thermal stability test in which selected capacitors were operated at high repetition rate into a low impedance load.

Because of the interest in high repetition rate duty for capacitors evaluated in this program, and because of the illustration of the thermal problem afforded by the thermal stability test, an example of this portion of the initial quality testing is singled out here. The thermal stability test is dynamic in nature, since it involves charging and rapid discharging of the unit under test. However, the dynamic testing carried out in this program has been defined more restrictively to tests carried out in vacuum with a simulated plasma thruster load. Dynamic tests of this kind are reported in the next section.

The purpose of thermal stability testing is to eliminate from further testing, those units which show indications of catastrophic failure. A catastrophic failure would occur for example if the power factor of the test sample were to rise with temperature and time at a rate which would cause the sample to generate more losses than it could dissipate within the design limits of the capacitor. A unit is considered to be thermally stable if it can be shown that the equilibrium temperature that the unit will reach ultimately is within the maximum specified limits of the materials used to fabricate the sample. A thermal stability curve is a plot of average temperature rise versus time for a sample unit operated under a given set of conditions. From the data collected a typical temperature rise versus time curve is evolved. Using the curve new units may be evaluated for thermal stability properties on a short time basis. Once a particular capacitor geometry is chosen, the thermal stability apparatus may be used to evaluate various capacitor materials on a normalized basis, and under quasi-dynamic operating conditions.

The thermal stability apparatus is essentially an RC relaxation oscillator. The entire apparatus consists of a power supply which charges the capacitor to a specified voltage, a charging resistor which together with the capacitance of the test sample determines the free running rate of discharge, a load design to simulate somewhat the actual load, and diagnostic equipment including voltage milliameters, a thermocouple potentiometer and a monitoring oscilloscope.

Figure 5 illustrates details of the portions of the apparatus which include the sample unit under test and the coaxial spark gap load. The load is a water-cooled coaxial spark gap. The anode and cathode members in contact with the plasma are made of silver for long wear and may be replaced in less than a minute. The remainder of the assembly is brass. The barrel is water-cooled by a copper coil soldered to the outer periphery of the barrel and located about 1 inch behind the gap. The purpose of the water cooling is to isolate the heat generated by the plasma from that heat generated by the capacitor under test in order to arrive at a truer representation of the capacitor's losses.

Based on preliminary thermal stability testing, a characteristic stability curve was deduced for a Mylar unit as shown in Figure 6. The

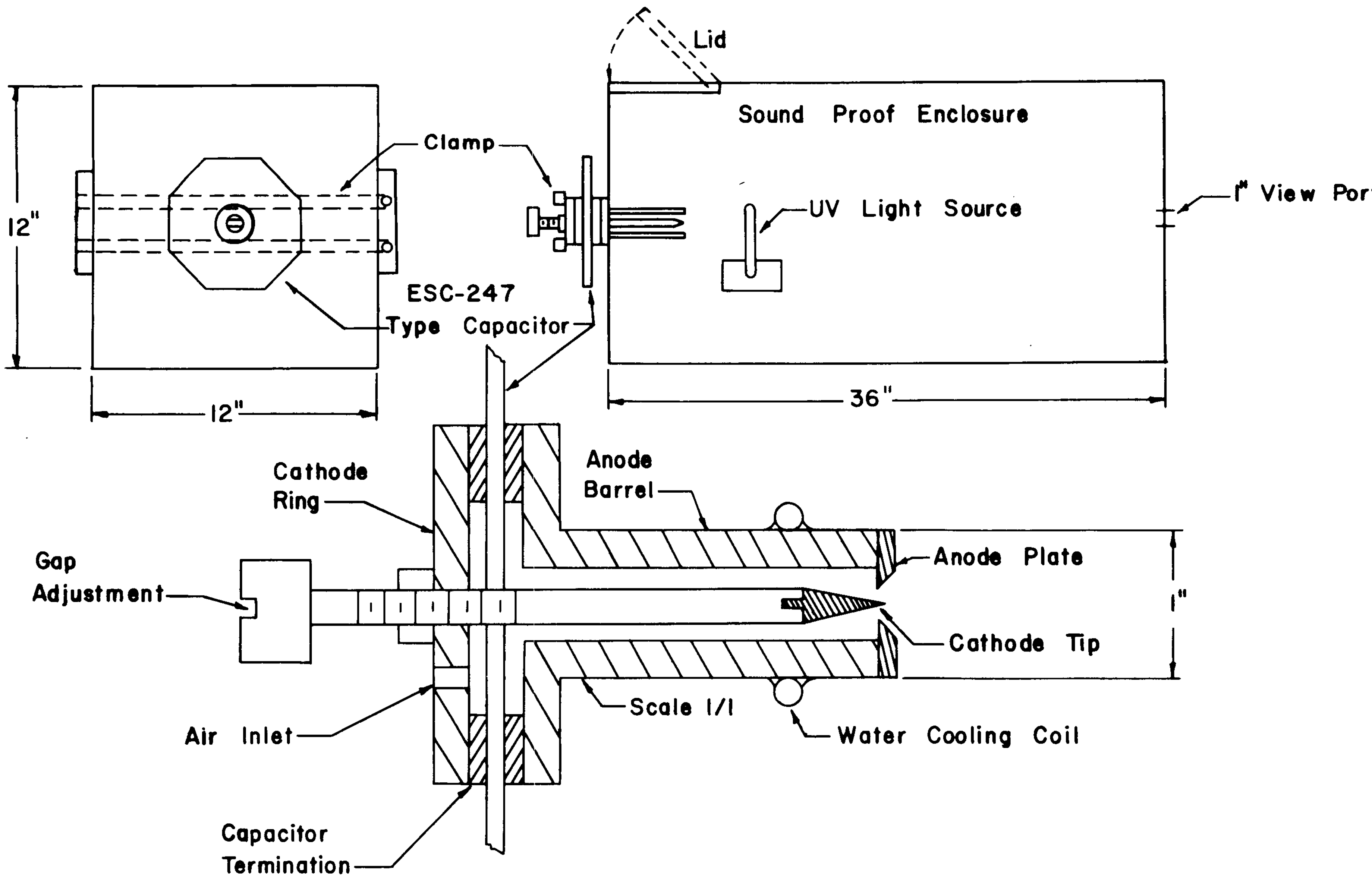

FIGURE 5

THERMAL STABILITY APPARATUS

21A-A1402

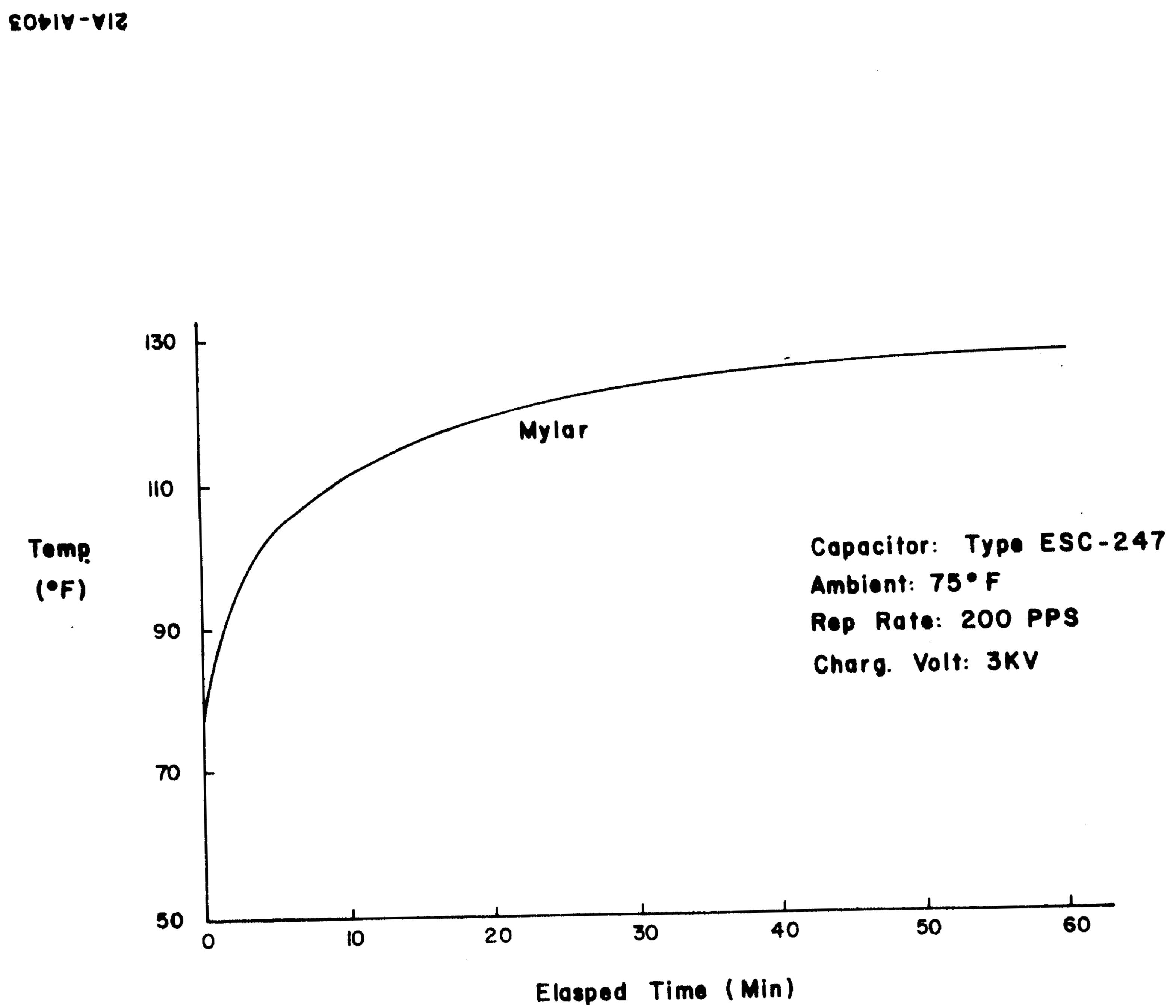

FIGURE 6

TYPICAL THERMAL STABILITY CURVE

following represents the test program used in all ESC-247 thermal stability tests.

1. The capacitor is charged to its rated operating voltage.

2. The temperature used to determine the thermal stability curve is the mean temperature readings of four thermocouples located at the mean capacitor radius.

3. The ambient temperature is recorded and will be the laboratory ambient temperature within three feet of the capacitor.

4. The air around the capacitor is still except for convection currents caused by the capacitor itself.

5. The discharge rate is chosen to cause a typical unit of the type being tested to reach an equilibrium temperature rise of fifteen to twenty-five degrees centigrade.

6. The capacitor is operated for a period of time necessary to determine beyond doubt that the unit is typical of its type and stable. For the Tobe Type ESC-247 capacitor the necessary amount of time is somewhere between 10 and 15 minutes.

3.3. Static Test Units

In the early portion of the program the experimental evaluation of capacitors centered around the ESC-247 production model flat disc capacitor which employed Mylar as dielectric material. Similar capacitors were fabricated in several combinations of dielectric thickness and foil material (aluminum or copper). As lamination methods were developed for Isomica, additional units were prepared using this material as dielectric. The make-up of units fabricated for static evaluation is given in Table III. The identification number designates the order in which the units were evaluated and is not indicative of the fabrication cycle. It is seen that all units employed foil thickness of 2 mils with either copper or aluminum for foil material. The third column of the table gives the number of dielectric layers employed as well as the dielectric thickness and material.

Each unit was fabricated in the basic ESC-247 geometry. Capacitance varied nominally from 0.05 to 0.10 microfarads. Measurements were

TABLE III

Static Test Units

Test Unit	Foil	Dielectric	Comment
1.	2 mil, Cu	1-layer, 5 mil Mylar	Standard ESC-247
2.	2 mil, Cu	1-layer, 5 mil Mylar	Standard ESC-247
3.	2 mil, Cu	1-layer, 5 mil Mylar	Standard ESC-247
4.	2 mil, Al	1-layer, 5 mil Mylar	
5.	2 mil, Al	5-layers, 1 mil Mylar	
6.	2 mil, Cu	2-layers, 2 mil + 3 mil Mylar	
7.	2 mil, Al	3-layers, 2 mil Isomica	First trial fabricated unit using Isomica
8.	2 mil, Cu	2-layers, 5 mil Mylar	
9.	2 mil, Cu	3-layers, 2 mil Isomica	
10.	2 mil, Cu	6-layers, 2 mil Isomica	

obtained of the basic capacitor parameters as a function of temperature over the range -50°C to the high temperature mechanical failure limit. These measurements included: (1) capacitance and dissipation factor at 1000 cps, (2) high frequency Q, (3) leakage resistance and (4) delamination and mechanical failure onset temperature. The importance of these determinations lies in the comparison of Isomica and Mylar as dielectrics. The results show clearly the superiority of Isomica especially in regard to high temperature capability. At the stage in the program when these measurements were performed, however, the techniques in manufacture of Isomica capacitors were not fully developed. Therefore, the results cannot be construed as final. For this reason, the data shown below are presented in summary form to indicate the trend and to make the salient comparisons in properties. Comparisons of aluminum versus copper as foil material showed no important difference except unit weight.

All of the following results were obtained statically (not involving capacitor discharge of stored energy) at atmospheric pressure. The thermal environment was maintained and controled by means of a temperature test chamber (Model 1060 WF, Delta Design, Inc.). Other instrumentation employed is identified or described along with the specific measurement cited below.

3.4. Capacitance and Dissipation Factor @1000 cps

Conventional Bridge measurements were carried out on all of the units listed in Table III at the bridge frequency of 1000 cps. The data obtained are tabulated in Table IV which lists capacitance for each unit as a function of temperature, and Table V which lists the dissipation factor at each temperature.

The measurements do not indicate any large difference dependent upon capacitor construction for units of similar dielectric material. However, there appears to be a trend toward lower dissipation factor at high temperature for the aluminum foil units. The large dissipation factor for Unit 7 was due to an incomplete cure of the unit during fabrication. That the results of that unit are not typical of Isomica capacitors is seen by

TABLE IV

Capacitance vs. Temperature @1000 cps

T(°C) \ Unit	1	2	3	4	5	6	7	8	9	10
-50	.0878uf	.0876uf	.0868uf	.0857uf	.0775uf	.0848uf	.1078uf	.0444uf	-	-
-30	.0894	.0895	.0884	.0872	.0792	.0862	.1078	.0450	.1002uf	-
-10	.0911	.0910	.0899	.0889	.0816	.0883	.1081	.0458	.1001	-
+10	.0924	.0922	.0910	.0903	.0841	.0899	.1083	.0465	.1015	-
+30	.0927	.0924	.0913	.0907	.0845	.0903	.1112	.0467	.1041	.0522uf
+50	.0929	.0927	.0914	.0907	.0845	.0905	.1126	.0468	.1038	.0520
+70	.0936	.0934	.0919	.0910	.0844	.0908	.1131	.0470	.1034	.0519
+90	.0952		.0941	.0927	.0850	.0927	.1118	.0479	.1031	.0516
+110	.0971*								.1025	.0512
+130									.1018	.0505
+150									.1003*	.0490*

*Onset of failure characterized by temporal increase in dissipation factor and decrease in capacitance.

TABLE V

Dissipation vs. Temperature @1000 cps

T(°C) \ Unit	1	2	3	4	5	6	7	8	9	10
-50	1.23%	1.35%	1.34%	1.37%	1.48%	1.50%	0.15%	1.45%	-	-
-30	1.08	1.22	1.20	1.21	1.32	1.39	0.24	1.35	.15%	-
-10	0.97	1.08	1.09	1.12	1.39	1.25	0.60	1.15	.13	-
+10	0.57	0.70	0.71	0.70	1.19	1.15	1.20	0.85	.10	-
+30	0.26	0.39	0.42	0.41	0.48	0.51	2.25	0.45	.10	.13 %
+50	0.25	0.40	0.45	0.22	0.30	0.48	2.70	0.35	.13	.17
+70	0.62	0.72	0.65	0.24	0.31	0.79	2.75	0.46	.16	.25
+90	1.20		1.49	0.92	1.05	1.74	2.75	0.99	.18	.33
+110	2.20*								.19	.31
+130									.20	.31
+150									.10	.35

* Onset of failure characterized by temporal increase in dissipation factor and decrease in capacitance.

noting the results for Units 9 and 10.

Summarized results for capacitance are illustrated in Figure 7 in which Mylar and Isomica are compared. The ordinate is the measured capacitance relative to the room temperature value, C_o. The onset of mechanical failure (delamination) is noted in the figure. A discussion of this comparison is given below, but it is clear at this point that even the prototype Isomica capacitor tested has a higher temperature capability in this respect than the Mylar unit. The principal difference in the capacitance versus temperature characteristics lie in the variation above room temperature where the Isomica unit shows a decrease at elevated temperature, while Mylar increases in the same range. Also, the magnitude of the variation is somewhat less in Isomica.

Measurements of dissipation factor are summarized in Figure 8. The figure illustrates one of the characteristics of Isomica which makes it an excellent capacitor material. The two-fold characteristic is that the low frequency dissipation factor is considerably lower for Isomica as compared to Mylar and that the variation with temperature is much less for Isomica. Since the quantity measured is the low frequency (1000 cps) dissipation factor, the practical significance to the program is in relation to the energy loss during charging at the intended repetition rates. The dissipation factor is the fraction of the charging energy which is dissipated as thermal energy in the unit. The results shown indicate that this energy loss is negligible for Isomica even at elevated temperature compared to the high frequency losses.

3.5. Leakage Resistance

Leakage resistance was measured at 300 volts by means of a battery connected in series with the capacitor under test and an ultra-sensitive microammeter (R.C.A. Model WV-84C) which permitted current measurement down to 10^{-9} amperes. Leakage resistance as high as 10^{11} ohms could be readily measured. Capacitor temperature was maintained and controlled by means of the thermal chamber described above.

Results for Mylar and Isomica dielectric in the ESC-247 capacitor

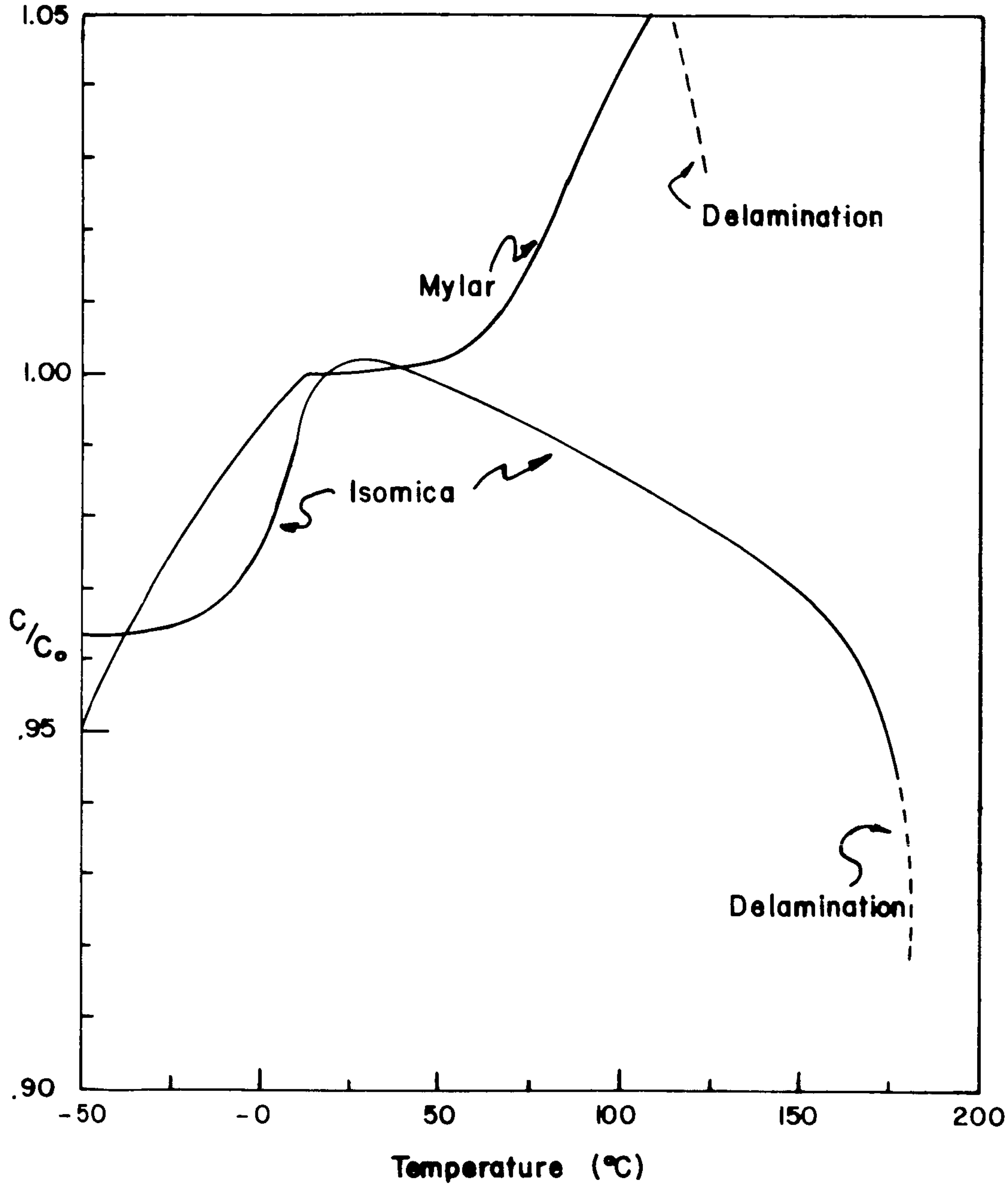

FIGURE 7

THERMAL VARIATION OF CAPACITANCE IN MYLAR AND ISOMICA ESC-247 CAPACITORS

21-A1162

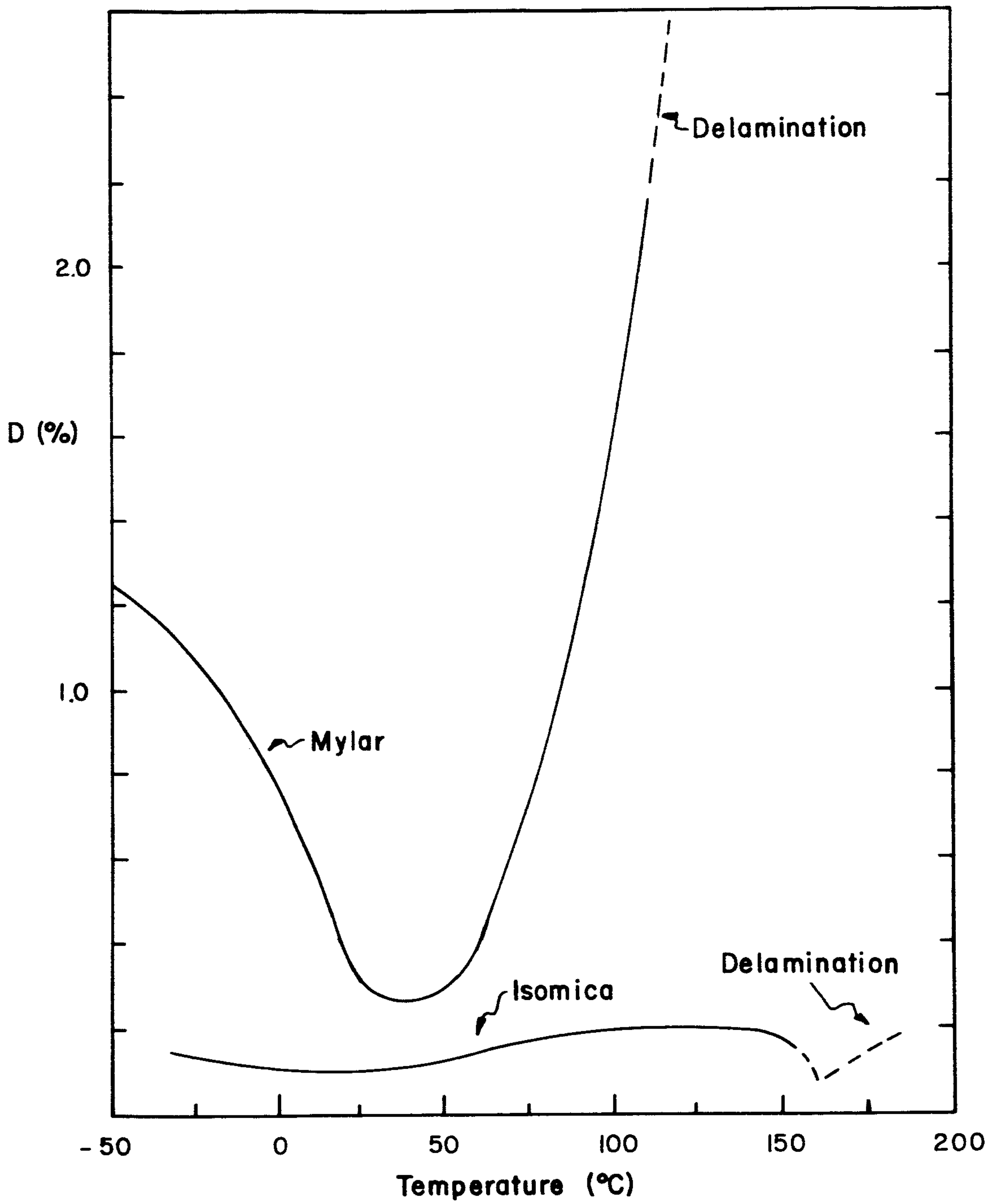

FIGURE 8

THERMAL VARIATION OF DISSIPATION FACTOR IN MYLAR AND ISOMICA ESC-247 CAPACITORS

21-A1163

configuration are compared in Figure 9 in which the time constant RC has been plotted against temperature. The results for Mylar are characteristic of capacitors fabricated from this material. It is interesting to note that the time constant is approaching values as low as a few seconds in the temperature range where other results indicate general failure of the capacitor. The Isomica unit has nearly the same time constant as the Mylar unit at room temperature but the decrease at high temperatures is at a much reduced rate.

The significance of the leakage resistance in terms of a power loss mechanism was discussed in Section 2. In high repetition rate applications, the time constant for loss of charge is important only if comparable to the repetition frequency. The fundamental significance of the time constant RC lies in the fact that it is determined by the dielectric constant and resistivity of the dielectric material itself and does not depend upon capacitor construction details.

3.6. High Frequency Q Measurements

The effective series resistance of the test capacitors under study is very low (a few milliohms) at frequencies in the megacycle range. In measurements of the high frequency Q, therefore, a method was developed which circumvents some of the difficulties encountered in usual bridge measurements at these frequencies. The technique consists of attaching a load whose series AC resistance is easily calculated and whose inductance is such that it provides a resonant frequency in the range of special interest. The standardized load which has been fabricated for this purpose is illustrated in the sketch of Figure 10. The material used throughout is copper except for the terminations. Because the load is coaxial, the currents which flow in it and in the capacitor are symmetrical, an important factor in obtaining meaningful results.

In operation oscillatory currents are generated in the load by means of a small mutual inductance as shown. This consists of a small wire loop placed in the region between the inner and outer conductor of the load. A high current pulse is derived from a capacitor discharge switched by

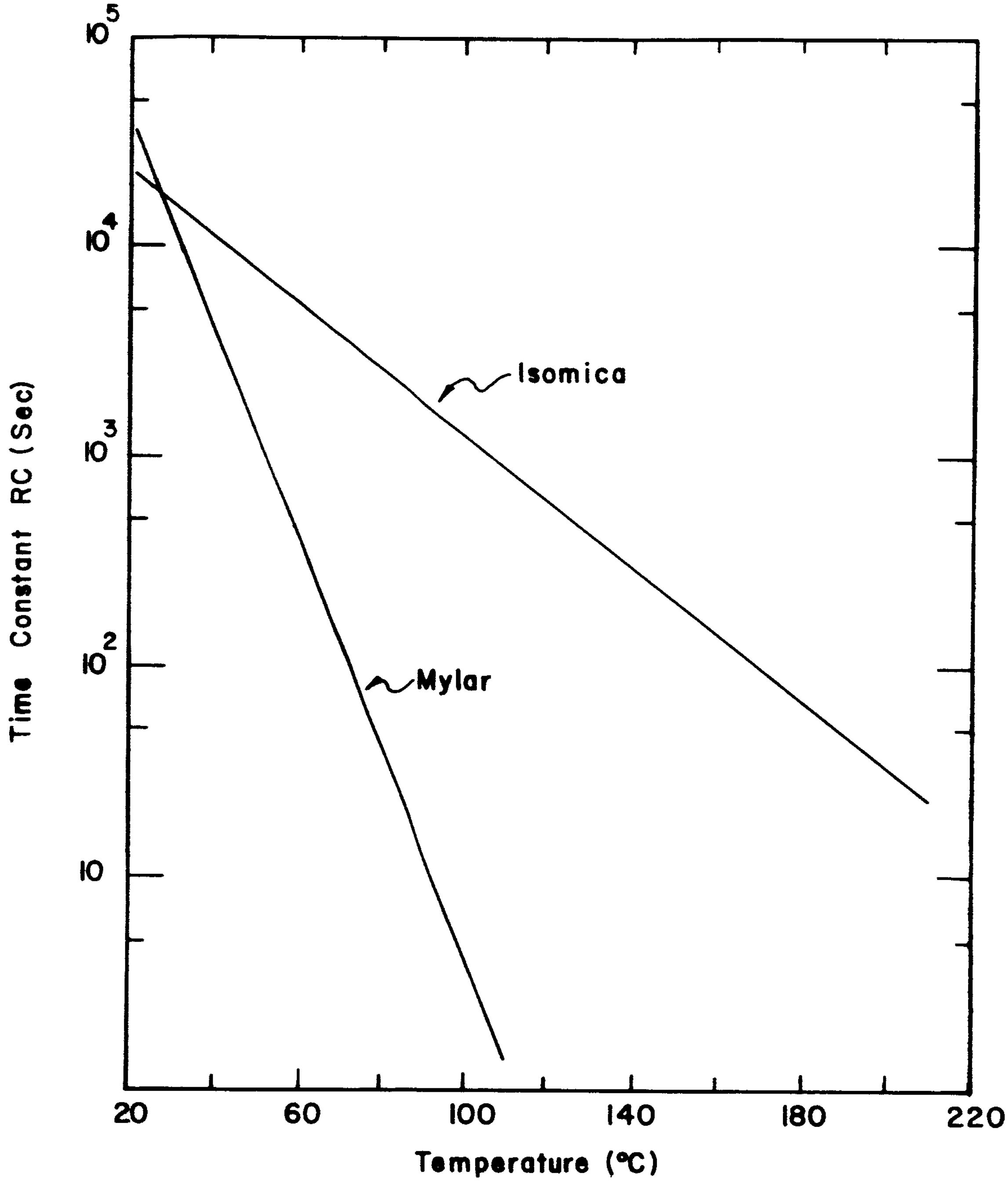

FIGURE 9

LEAKAGE RESISTANCE IN MYLAR AND ISOMICA
TYPE ESC-247 CAPACITORS

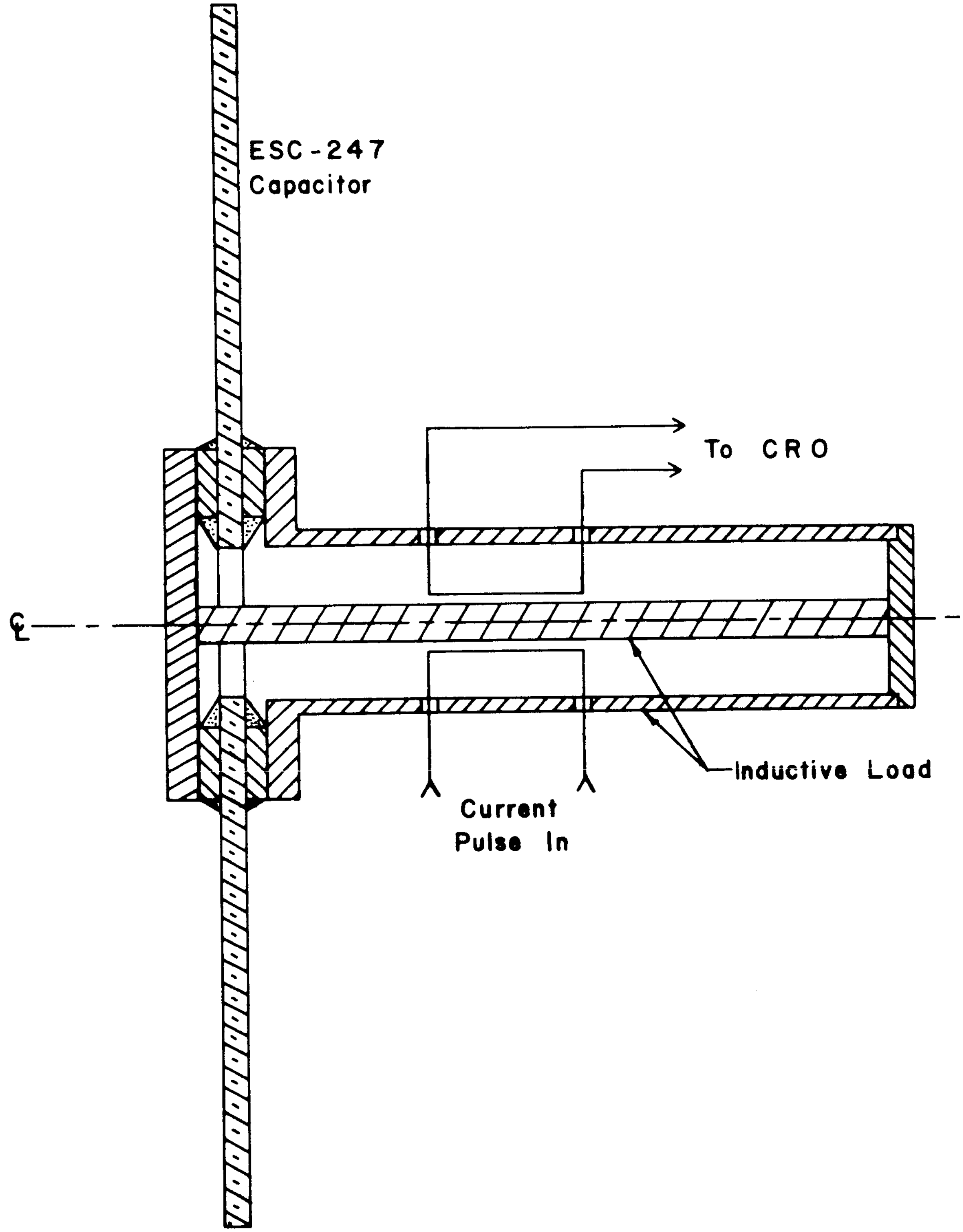

FIGURE 10. HIGH FREQUENCY Q MEASUREMENT TECHNIQUE

21-A1165

means of a thyratron. The driving pulse is essentially exponential in form and is short compared to the ring-down time for oscillations induced in the resonant circuit. The mutual inductance similar to the driving loop is used as a pick-up to display the damped oscillations induced. Q measurements for the capacitor under test with the standardized load are obtained by noting the damping over several cycles.

The self-inductance of the test load is 2.8×10^{-8} henry, providing a ringing frequency, when testing the ESC-247 type units, of about 3 MC depending on the actual capacitance of the unit under test. The series AC resistance, attributable almost exclusively to the center conductor (because of its small circumference), is 2.28×10^{-3} ohms at room temperature.

Adjusted values of Q for two tests units are shown in Figure 9 as a function of temperature. Adjustment refers to the fact that the load resistance is subtracted from the over-all effective series resistance and a new value of Q is computed which would apply if the external circuit had no resistance.

Two curves are shown in Figure 11. The lower figure is typical of the Q values and variations with temperature which characterize all of the Mylar test units. The resonant frequency of the particular Mylar unit tested with the above load was 3.04 MC as noted. The Isomica unit is seen to have a much higher Q at high frequency than the comparable Mylar models. Also, there is an apparent difference in the temperature variation. Because of the slightly higher capacitance of the Isomica unit, the observations were obtained at a lower frequency, as noted.

3.7. Capacitor Failure at Elevated Temperature

Several of the test units were intentionally failed at high temperature to permit an examination of their failure characteristics. High potential testing at elevated temperature revealed that the principal failure mode was not related to weakening of dielectric strength, but was associated with loss of mechanical integrity through warping and delamination.

Short term failure in the standard Mylar unit was observed to occur at 110°C where there arose a temperal decrease in capacitance (indicative

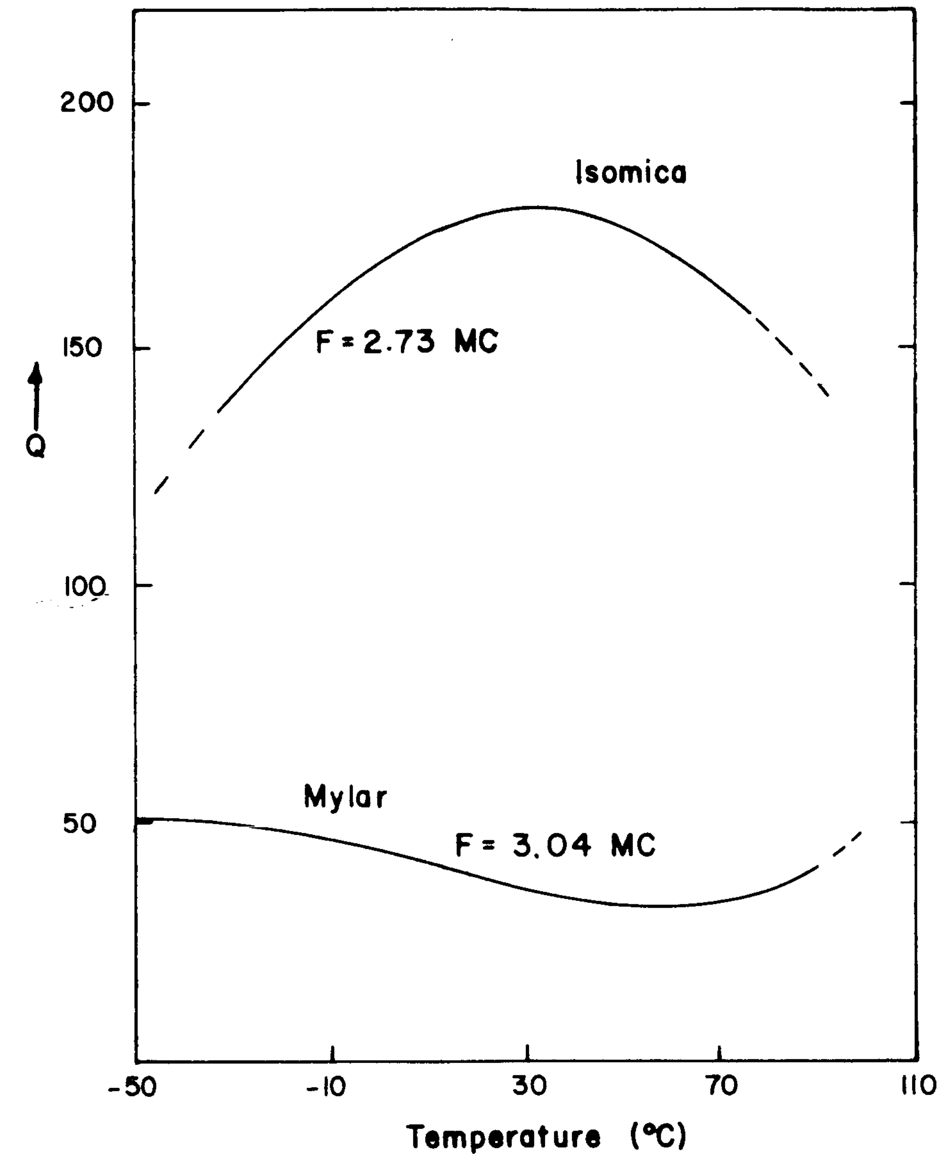

FIGURE 11

HIGH FREQUENCY Q MEASUREMENTS

of delamination) and an increase in dissipation factor. After 30 minutes at this temperature the capacitor exhibited a slight deformation at the outer radius of the foils. An increase of temperature to $120^{\circ}C$ produced severe delamination and the softened Mylar was seen to curl and warp substantially.

An investigation of the long term failure in Mylar revealed a more subtle onset of mechanical failure at somewhat lower temperatures than those cited above. Results of a 48 hour test at a maintained temperature of $90^{\circ}C$ showed a slow degradation of capacitor properties. This was evidenced by a gradual decrease in capacitance and fluctuations in the dissipation factor. The latter is attributed to the build-up and removal of volatiles in the unit. A quantitative measure of the observed deformation is provided by the capacitance decrease which was approximately 3% over the period of the test. A log of the 48 hour test in Mylar Unit 8 is given in Table VI, which presents the values of dissipation factor and capacitance (both obtained at 1000 cps) at various temperatures up to $90^{\circ}C$. The elapsed time after the capacitor temperature reached $90^{\circ}C$ is also indicated in the table.

The failure mechanisms in Isomica due to elevated temperature are in sharp contrast to those noted above. While the high temperature capability is clearly above Mylar, the limits described here are thought to be indicative of the method of fabrication at the particular stage of development. It is suspected that the failure limits of capacitors made under recently improved techniques are at even higher temperature, although this has not been confirmed.

The results of a single destructive run for Unit 9 are illustrated in Figure 12. In the figure both dissipation factor and capacitance are plotted against temperature. These data were obtained at approximately 30 minute intervals which is the time required for thermal equilibrium between the capacitor and the thermal chamber. The onset of failure occurs just above $140^{\circ}C$ where a temporal decrease in capacitance is noted together with a spurious decrease in dissipation factor. Further

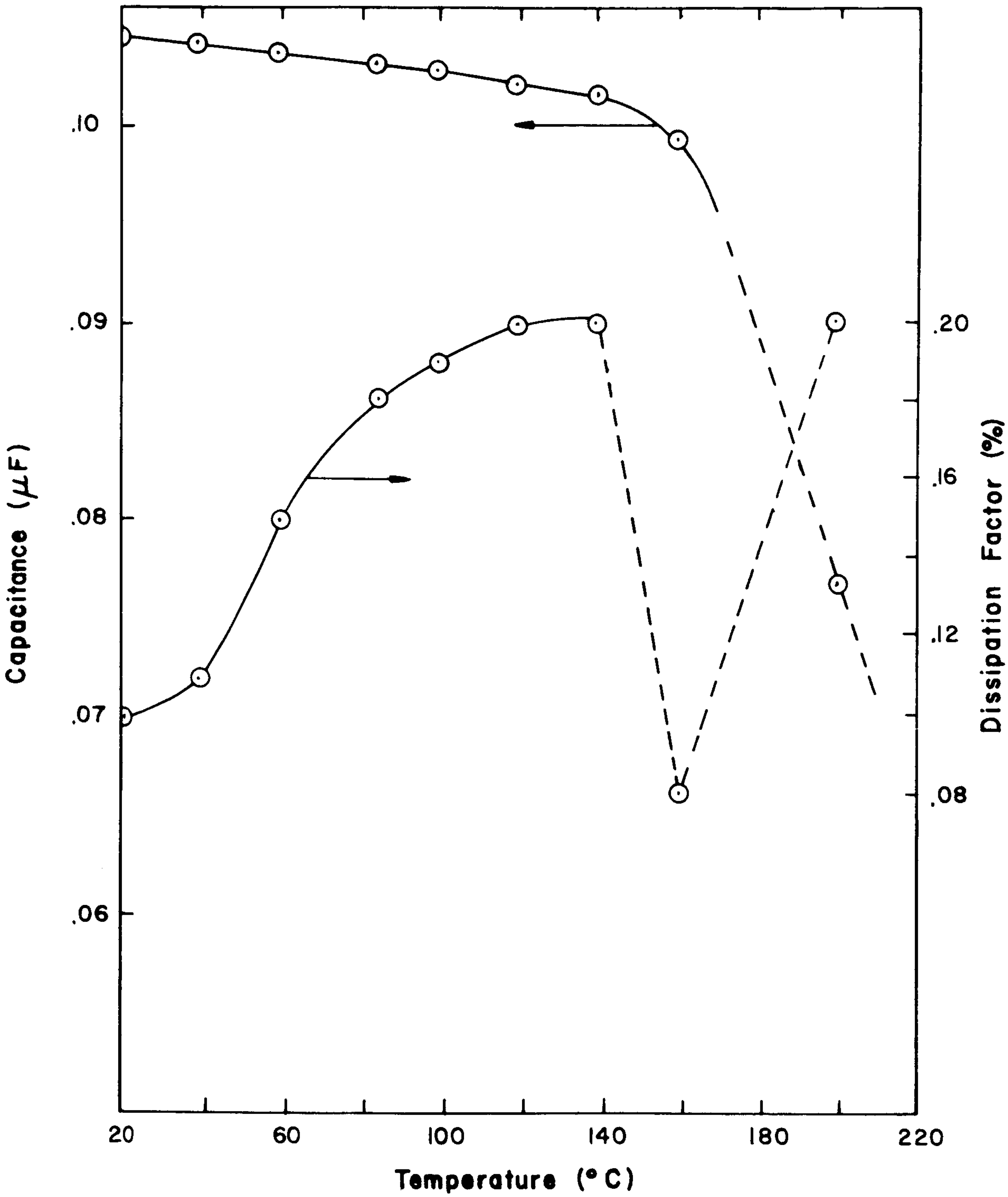

FIGURE 12

HIGH TEMPERATURE EFFECTS IN AN ISOMICA TYPE ESC-247 CAPACITOR

21A-A1404

TABLE VI

Long-Term Variations in a Mylar Capacitor at Elevated Temperature

Temp.(°C)	D(%)	C(µf)	Time (Hrs)
-50	1.45	.04440	-
-30	1.35	.04505	-
-10	1.15	.04581	-
+10	.85	.04648	-
+30	.45	.04667	-
+50	.35	.04675	-
+70	.46	.04695	-
+90	.99	.04785	0
+90	1.05	.04785	2
+90	1.05	.04775	3
+90	1.05	.04775	4
+90	1.05	.04775	5
+90	1.07	.04759	6
+90	.95	.04675	22
+90	1.00	.04660	29
+90	.90	.04610	46

increase in temperature results in a large decrease in capacitance accompanying delamination of the unit. Gross deformation previously observed for Mylar test units is notably absent even after temperatures of 250°C are obtained. The Isomica unit retains its initial form and stiffness so that mechanical failure is characterized by delamination alone. It is expected, therefore, that improved fabrication methods can yield a capacitor capable of maintaining mechanical integrety at these higher temperatures.

Unit 10 was an Isomica unit similar in design to Unit 9 except that six 2 mil layers of dielectric were laminated between each copper foil pair. Measurements of dissipation factor and capacitance for this unit were carried out to investigate the effects of temperature cycling on failure. The thermal cycle was as follows:

The temperature was elevated to 100°C in 20°C steps and maintained for 30 minutes. The temperature was then increased to 120°C and maintained for 30 minutes noting the slight parameter changes. After thermal equilibrium was attained at 140°C the unit was permitted to cool to 100°C. The temperature was then raised to 140°C and 160°C before cooling to 100°C. This was repeated and extended to 180°C which was maintained for 30 minutes while a temporal decrease in capacitance was noted before cooling again to 100°C. Finally, the temperature was elevated to 200°C and the unit was allowed to cool.

The results are illustrated in Figure 13, in which capacitance is plotted versus temperature. Data were obtained during the heating portions of the various cycles as indicated. The dashed lines indicate approximate cooling curves. The degradation of the capacitor is evidenced by the decreasing capacitance values at 100°C after each excursion of the unit to higher temperature.

Measurements of dissipation factor which accompanied the capacitance measurements indicated a gradual decrease in dissipation during each cycle. For example, dissipation factor decreased from an initial

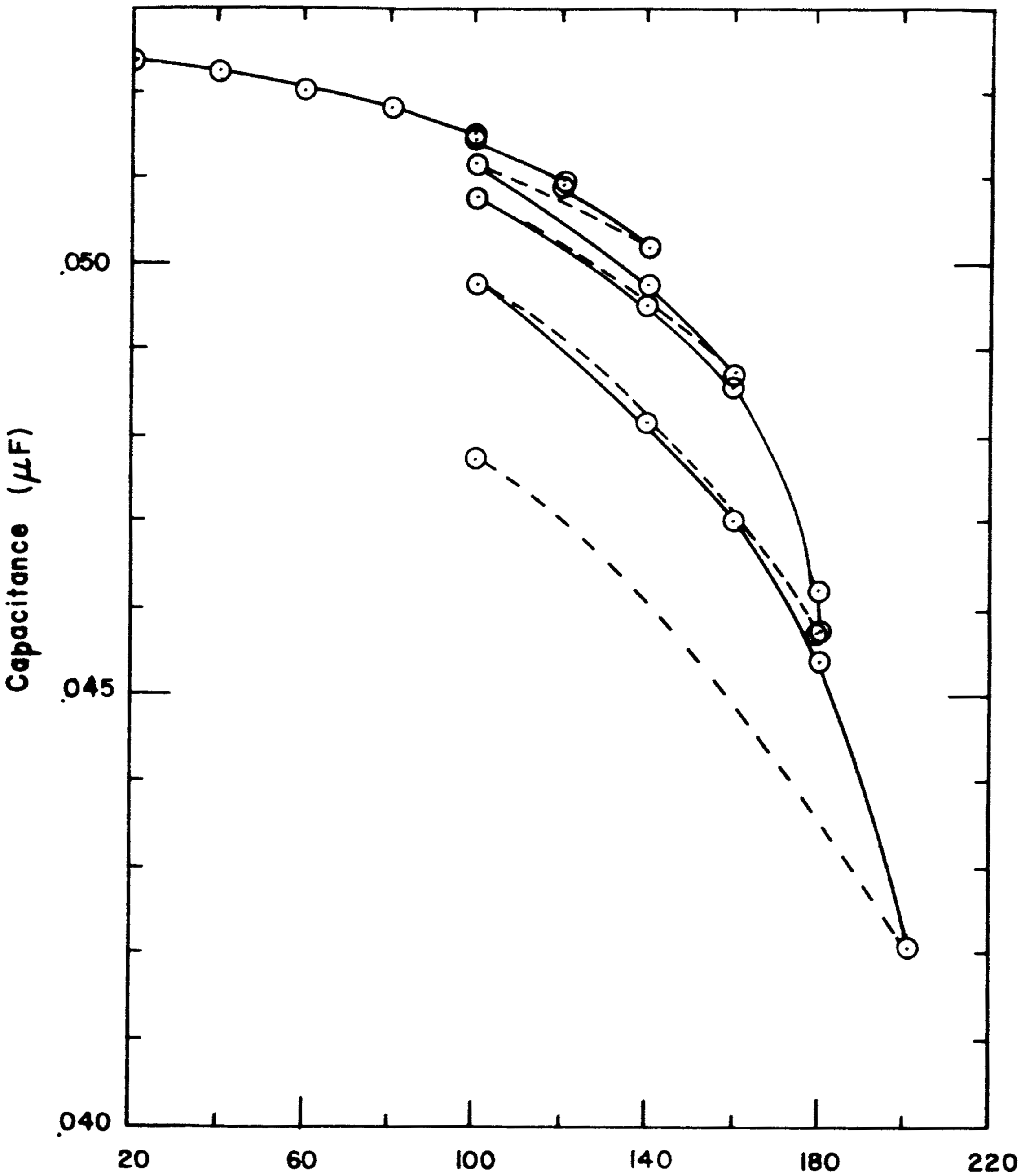

FIGURE 13

TEMPERATURE CYCLING EFFECTS IN AN ISOMICA TYPE ESC-247 CAPACITOR

21A-AI405

$100^{\circ}C$ value of 0.37% to 0.05% at the conclusion of the thermal cycling.

3.8. Conclusions

Analysis of self-generated heat in energy discharge capacitors used in high average power applications has pointed to the need for a high temperature capability. A high operating temperature is necessary if the storage system is to radiate self-generated heat, while the latter is minimized if the capacitor has a high Q.

A material which appears to have considerable advantage in these regards is Isomica. In the measurements carried out above, Isomica has been compared with the more conventional dielectric material, Mylar. While laminated capacitors fabricated of Mylar are suitable for operation up to $90^{\circ}C$, the tested Isomica units could operate successfully at temperatures up to $140^{\circ}C$.

In view of the nature of the mechanical delamination of these units, it is reasonable to speculate that improved lamination methods would yield a successful $200^{\circ}C$ Isomica capacitor.

At elevated temperatures, Isomica units exhibit a much higher leakage resistance and much less dissipation at both high and low frequencies as compared to Mylar capacitors of the same mechanical design.

These conclusions were reached early in the program. As a result, the improvement of lamination techniques were applied to the construction of 24 inch ESC-247 capacitors. The remainder of the evaluation program then dealt with the dynamic performance of these larger units as described in the remainder of this report.

4. Capacitor Evaluation (Dynamic Testing)

4.1. Approach and Instrumentation

Evaluation of the ESC-247-C capacitor was carried out under conditions which were designed to simulate actual operating conditions with regard to electrical load and environment. The evolution of these units and their scaling from the smaller ESC-247 capacitor has been traced in Section 2. Paralleling the effort to develop a successful Isomica capacitor was the design and assembly of a suitable system for dynamic evaluation. The developed system employs a simple coaxial plasma gun designed specifically to provide a reasonable simulation of the load characteristics of pulsed plasma thrustors currently envisioned for advanced propulsion systems. One of the principal attributes of the developed gun is the method of triggering the plasma discharge which permits an accurate control of the discharge repetition rate.

The dynamic evaluation system was designed to provide thermal isolation of the capacitor and plasma gun from the environmental chamber. The function of the latter is to reduce the importance of convective cooling, thus limiting the heat loss from the capacitor to radiative loss alone. Under these conditions it has been possible to evaluate heat sources and thermal distributions with some confidence.

During the dynamic evaluation phase, considerable progress has been seen in the successful fabrication of large Isomica capacitors. While the first units tested were failed mechanically by the vacuum environment alone, the last units tested have been characterized by an operating life which exceeds the continuous duty period of the plasma gun.

The experience gained in the dynamic evaluation phase has had several important by-products with regard to high repetition rate duty of the capacitor-plasma gun mating in vacuum. In addition to the desired information regarding factors effecting capacitor life and performance, light has been shed on the special problems of plasma gun triggering, insulator decomposition by corona within the gun and the relationship of deionization time in the plasma created to the repetition rate.

The dynamic evaluation apparatus is illustrated schematically in Figure 14. The basic elements of the apparatus include the environmental chamber in which the plasma gun and capacitor are mounted, the capacitor charging power supply, the triggering system and gas flow controls and the various diagnostic instrumentation.

The plasma gun and capacitor are mounted within the 30 inch vacuum chamber as indicated in Figure 15. The mechanical support includes a section of pyrex pipe as shown which serves to isolate the plasma gun thermally from the vacuum enclosure. Pressure in the chamber during operation is normally maintained below 10^{-4} mm-Hg to eliminate convective heat loss. The plasma gun is exhausted into a pyrex envelope containing the working gas (helium or argon) at pressures in the range of 25 to 150 microns Hg. The purpose of this enclosure is to insure that the plasma gun is immersed in a reservoir (approximately 20 liters) of the desired working gas. Gas flow is through the central electrode of the plasma gun as described below in conjunction with the gun design. The output flow is through a small throttling valve to the main vacuum chamber. Working gas reservoir pressure is adjusted by means of this valve and a controlled leak valve in the input line.

Power is derived from a 75 kilowatt, 0 to 15 kilovolt DC power supply. In all of the reported operation negative polarity output was employed. Resistance charging was used with a 15 K ohm power resistor immersed in a water-cooled oil bath.

Both flanges of the plasma gun were cooled by means of a forced circulating oil system. Copper cooling coils attached to the gun flanges were interconnected with insulating tubing for high potential isolation. An oil-to-water heat exchanger was employed external to the vacuum enclosure to limit the temperature rise of the oil reservoir.

Temperature measurements at several locations on the capacitor and within the oil cooling lines were accomplished by means of copper-constantan thermocouples. The detailed deployment of thermocouples is specified below in connection with the thermal measurements.

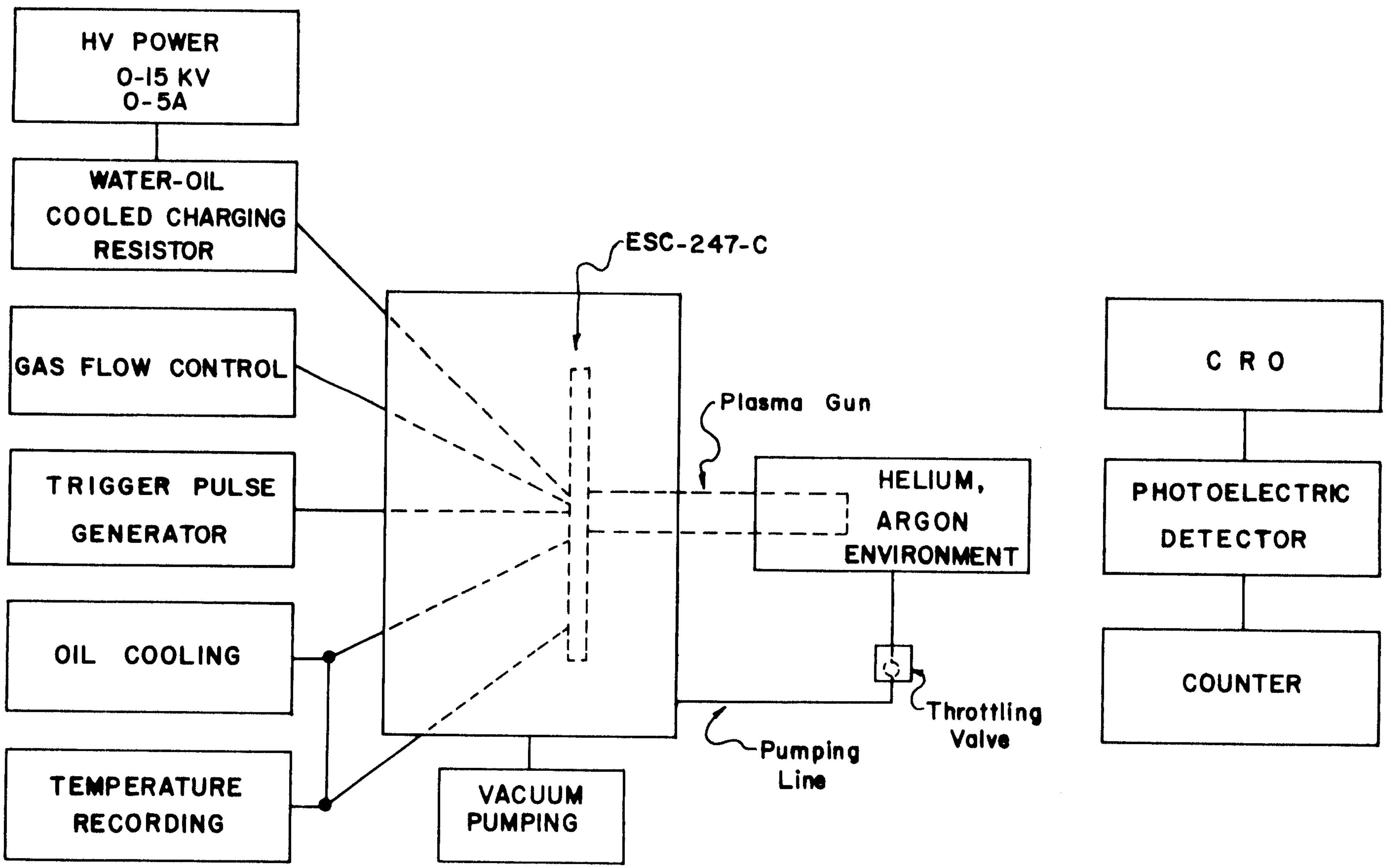

FIGURE 14

DYNAMIC EVALUATION APPARATUS

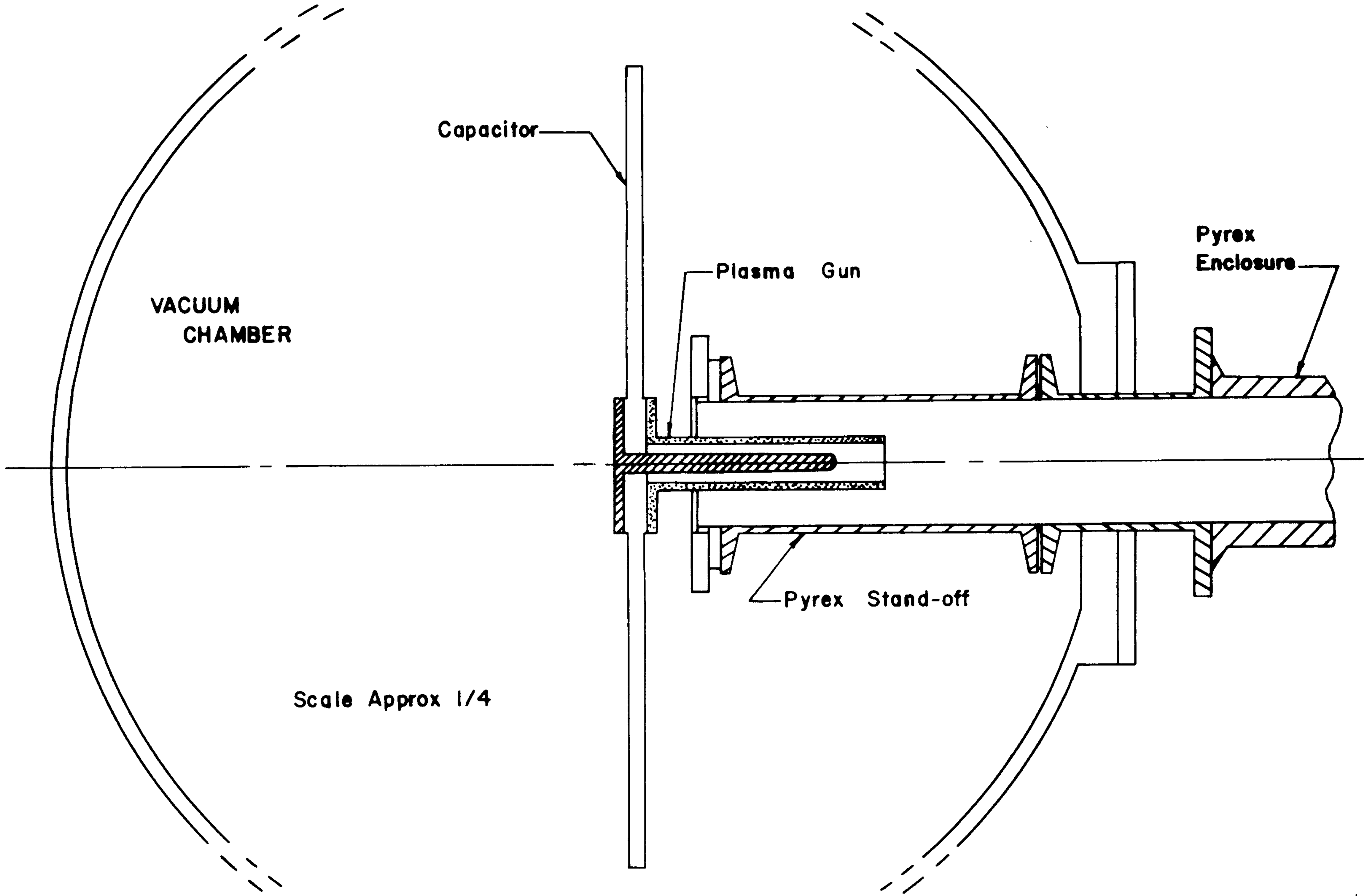

FIGURE 15
PLASMA GUN MOUNTING

21-A1168

Temperature readout was by means of a single channel chart recorder preceded by a multiple position thermocouple switch. Observations of the discharge light pulse were made by means of a photoelectric detector which was also employed with a counter to record the discharge repetition rate and the total discharges accumulated during a continuous operation. Discharge waveform was observed by means of a small pick-up loop installed near, but external to the plasma gun.

Two of the key elements of the dynamic evaluation apparatus include the plasma gun and the method of obtaining accurately controlled repetition rates. The design of the gun and the method of triggering are described in the following paragraphs.

The plasma gun was designed for this program with the purpose to simulate some of the load characteristics of typical pulsed plasma thrustors. The capability to develop thrust was incidental to the design and performance in this respect was not evaluated within the program. The basic characteristics which it was designed to simulate were centered around the waveform properties of a pulsed plasma discharge. These include the damping characteristics, the starting transients, and the voltage transients associated with current reversals, current interruption, and time varying circuit inductance. Other than providing simulation, the employment of the plasma gun has led to a number of interesting observations pertinent to high repetition rate discharges at low pressure, and to a method for reliable triggering for controlling repetition rate to rates higher than 1000 pps. The performance evaluation of the gun and the problems encountered are considered in detail in a later section.

In this section the gun design is described for the gun in use at the conclusion of the program. A full-sized cross-section is illustrated in Figure 16. The gun employs coaxial copper electrodes connected as shown to the capacitor terminals by brass mounting flanges. Prior to assembly, the through-hole region of the capacitor is prepared by sealing in a heavy walled pyrex sleeve by means of a high temperature epoxy. The epoxy resin

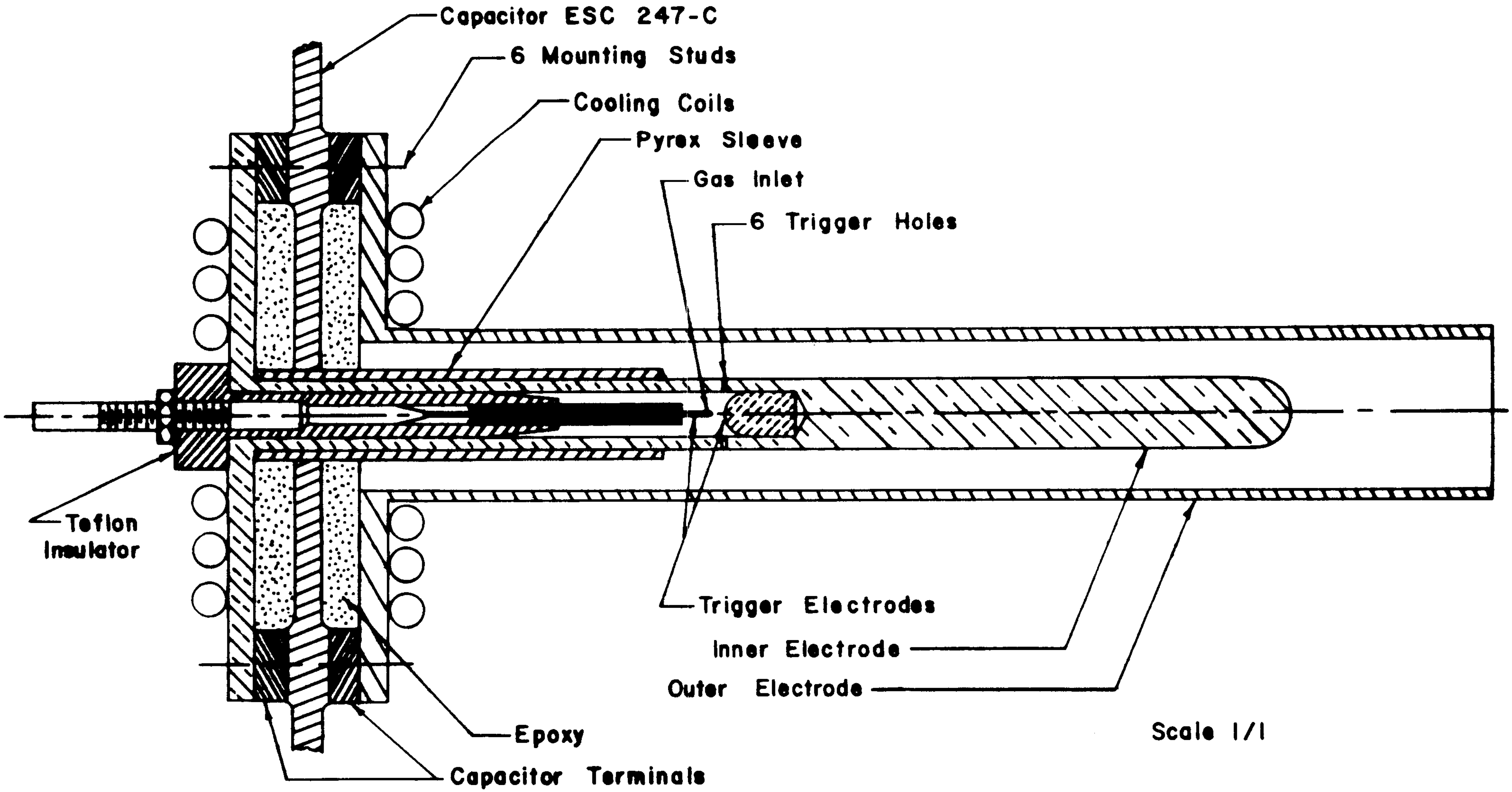

FIGURE 16

CROSS SECTION OF PLASMA GUN

used for this purpose is filled with alumina powder so that the cured material approximates the electrical properties of the ceramic. The pyrex sleeve provides breech insulation to the point along the center conductor where the discharge is initiated. The factors which led to this technique are discussed in the evaluation of the gun performance below.

The method for triggering the discharge makes use of trigger electrodes employed internal to the center electrode of the gun. One trigger electrode is a steel plug which is pressed into a center bore within the center electrode of the plasma gun. The second trigger electrode is insulated from the plasma gun as shown. Trigger pulses derived from a specially designed pulse generator are applied to this electrode causing a small discharge in the gas within the central electrode of the gun. The plasma which forms is ejected through six equally spaced holes (.028 in diameter) into the space between the electrodes of the plasma gun. The main discharge is then initiated at six locations around the center conductor thereby enhancing the chances of a spatially uniform plasma formation. Gas input flow is through the hollow trigger electrode so that the trigger discharge volume is at a pressure somewhat above that within the gun itself. This factor serves to enhance the breakdown for the initiating trigger pulse.

Because of the need for controlled high repetition rate operation in the dynamic system, the method for triggering the plasma gun has received special attention. The trigger electrode geometry has been described previously as an integral part of the gun design. The triggering circuit was developed in the course of preliminary dynamic testing and is described below.

The purpose of the trigger is to provide a sufficient number of initial electrons in the breech of the plasma gun to initiate breakdown leading to discharge of the stored energy. In accomplishing this it is desirable for the trigger spark to be of short duration relative to the acceleration phase of the main discharge in order to obviate multiple triggering. There is the additional requirements that minimal coupling capacitance exist between the high voltage terminal of the main storage capacitor and ground. The triggering scheme which has proven successful in these regards employs a coaxial cable to provide both the coupling and the energy storage required for the initiating spark.

The trigger circuit is illustrated schematically in Figure 17. The braid of a 100 ft. length of RG-8 is charged to a high potential, typically +7.5 KV, by a positive high voltage supply. The braid is then discharged at the desired rate by means of a 6279 hydrogen thyratron through 50 ohms to ground. The high voltage pulse induced in the center conductor then propagates along a short length of connecting cable (with grounded braid) to the trigger electrode. The pulse current is carried through the trigger gap to the inner gun electrode. The latter is effectively at AC ground in view of the capacitance of the energy storage capacitor. As described previously, the trigger spark so formed introduces ionization in the breech region of the plasma gun causing initiation of the main discharge.

The initial potential of the cable center conductor is referenced to the inner electrode by means of the resistance shown as 40 K ohms in the figure. During normal operation the center conductor is at the capacitor charging potential maintained by the main power supply.

In its final configuration the trigger pulse generator provides for manual push button and square wave generator inputs which are fed through a low voltage pulse forming network employing a 2D21 to the control grid of the 6229. The output pulses generated are 0.3 microseconds in duration with variable pulse height up to 10 KV. The circuit was designed for operation at pulse rates up to 1000 pps. However, it has functioned satisfactorily at rates up to 2000 pps.

4.2. Life and Failure Data

The first ESC-247-C units (Fabrication Cycles A through H) were generally unsuited for dynamic evaluation in that the delamination problem had not been overcome. These early units were used for testing certain portions of the dynamic facility design which required a capacitor in place. These tests included an evaluation of the triggering concept and gas flow

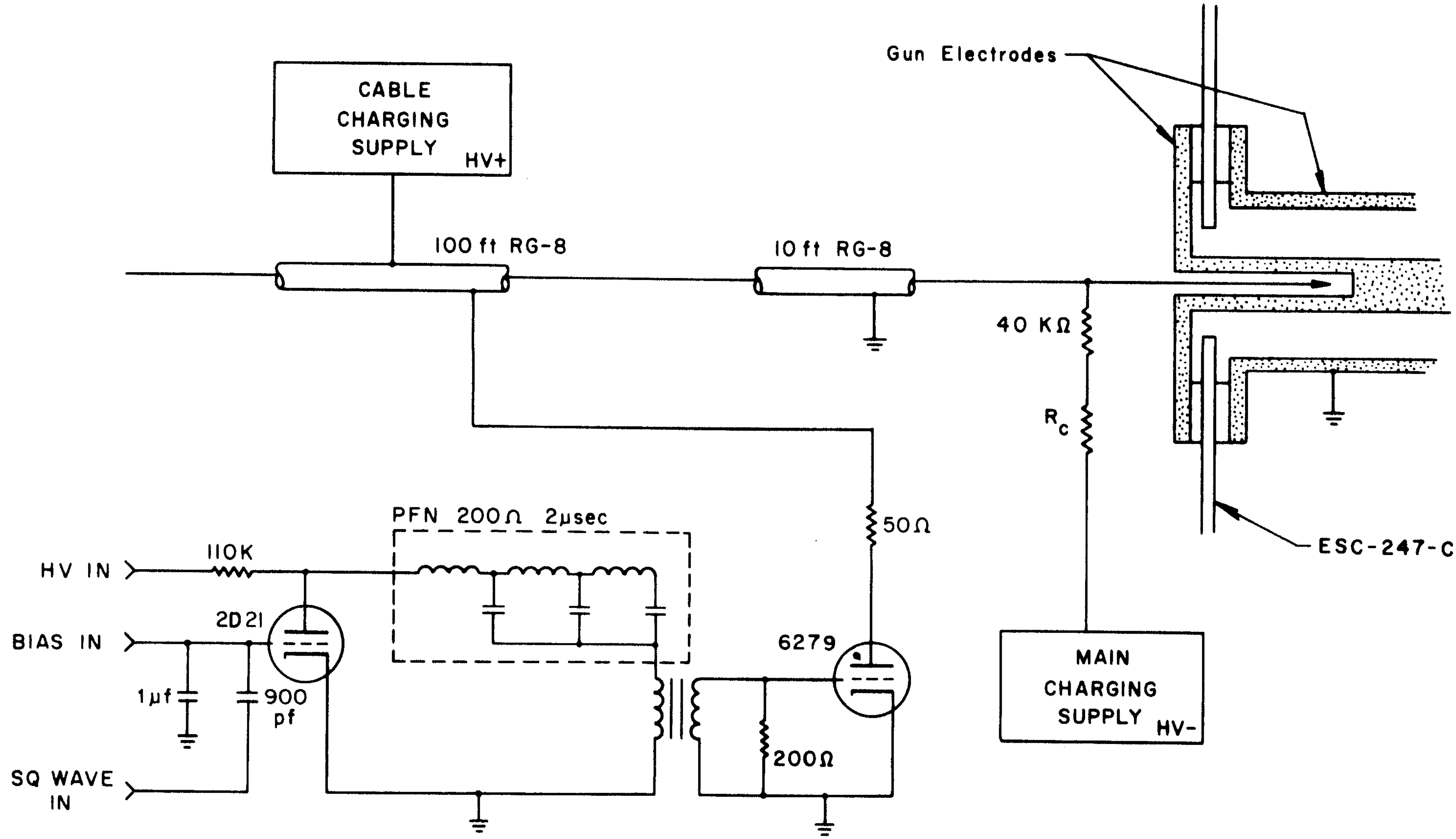

FIGURE 17

TRIGGER CIRCUIT

21-A2177

conditions in the system. It was also possible to assess the mechanical effects of vacuum environment on units which partially delaminated following manufacture.

Unit G was typical of those units which were in partially delaminated condition. An investigation of the effects of the vacuum environment demonstrated that the initial delamination is greatly amplified by the forces which develop due to trapped gas. This unit had an initial capacitance of 0.235 microfarads. When placed in a vacuum of 10^{-4} mm Hg, the capacitance decreased immediately to 0.191 microfarads. After eight hours at this pressure a further decrease to 0.169 microfarads was observed. When atmospheric pressure was restored, a value of 0.213 microfarads was measured illustrating the permanent increased delamination brought about by the vacuum environment. The unit did not withstand high voltage operation following the vacuum environmental test.

Unit I was the first unit fabricated with generally good lamination qualities. Capacitance decrease in vacuum was less than 1/2% of the initial value. In dynamic tests this unit withstood approximately 50,000 discharges prior to failure. Subsequent units showed steady improvement in mechanical properties as well as operating life.

Dynamic test conditions and information regarding duty, life and failures are summarized in the tabulations at the end of this section. The continuous duty period in minutes given in each table represents the duration of operation at the given pulse repetition rate without interruption. The terminal temperature given (in some cases) represents the temperature observed by a single thermocouple located at the junction of the capacitor terminal and the mating flange of the outer (ground potential) electrode of the coaxial plasma gun. The charging potential given is the actual capacitor voltage. Correction has been made, at the higher repetition rates, for the charging time constant, typically about five milliseconds. The charging resistance was 15.31 ohms in each case.

Regarding the failure information it is noteworthy that no dielectric punctures were observed throughout the program. All failures which occurred were along surface tracks in that portion of the capacitor internal to the terminals. In the early models this region was generally weak mechanically but was later improved through the use of dielectric inserts used to bring the thickness up to match that of the capacitor containing foil material. It was clear from the results obtained from Units J and K, that there was correlation between electrical failure and mechanical failure, the latter being brought about by elevated terminal temperatures. For this reason the plasma gun flanges were oil cooled beginning with dynamic evaluation of Unit L.

In addition to life data, a number of other observations were made during the sequence of tests. For example, Units I, J and K permitted an examination of gun and trigger performance and shed light on the problems of high repetition rate duty. The original gun design was modified on the basis of these findings. During Unit L testing, measurements were made of the radial temperature distribution. Units N and O operation led to information regarding ionization decay rates (of interest to high repetition rates) and calorimetric measurements employing a constant-flow method. These findings are summarized in Section 4.3 and 4.4, which deal with thermal measurements and gun performance respectively.

The following tabulations of operating duty for the various capacitors evaluated illustrate the marked improvement in capacitor quality during the course of the program. The last two capacitors evaluated represent a substantial stride toward obtaining program goals. Although subjected to much more severe duty than previous units, there has been no indication of electrical or mechanical failure of these units within the time limits of the program.

TABLE VII

DYNAMIC TESTS

UNIT I

Capacitance: 0.242 Microfarads

Charging Potential: 8.0 Kilovolts

Working Gas: Helium

Test Log:

Repetition Rate (pps)	Continuous Duty Period (Min.)	Total Discharges
< 10	20	50,000 (approx.)

Failure: Electrical breakdown along a surface track within the laminate near the terminations.

TABLE VIII

DYNAMIC TESTS

UNIT J

Capacitance: 0.240 Microfarads

Charging Potential: 8.0 Kilovolts

Working Gas: Helium and Argon as indicated

Test Log:

Repetition Rate (pps)	Continuous Duty Period (Min.)	Maximum Terminal Temp. (°C)	Working Gas	Total Discharges
15	40	79	He	36,000
15	30	83	A	27,000
30	30	113	He	54,000
Various	--	--	--	30,000
			Total	147,000

Failure: Failure was similar to that observed for Unit I. Failure occurred at peak terminal temperature of 113°C. The elevated temperature also initiated some slight delamination of the unit.

TABLE IX

DYNAMIC TESTS

UNIT K

Capacitance: 0.240 Microfarads

Working Gas: Helium

Test Log:

Repetition Rate (pps)	Charging* Potential (KV)	Continuous Duty Period (Min.)	Maximum Terminal Temp.	Total Discharges
2	5.0	63	34	7,500
5	5.0	48	43	14,500
10	5.0	180	65	108,000
20	5.0	147	72	176,000
50	5.0	9	--	27,000
100	4.5	6	100	36,000
			Total	369,500

Failure: Electrical breakdown along surface between Isomica and Epoxy near terminals, at peak temperature of 100°C. Extensive delamination also took place.

*Corrected for charging time constant ≐ 3.6 millisecond

TABLE X

DYNAMIC TESTS

UNIT L

Capacitance: 0.380 Microfarads

Working Gas: Helium

Test Log:

Repetition Rate (pps)	Charging Potential* (KV)	Continuous Duty Period (Min.)	Maximum** Terminal Temp. (°C)	Total Discharges
10	4.0	50	53	30,000
10	4.0	78	33	47,000
100	3.2	90	44	540,000
100	3.2	85	--	510,000
50	3.9	60	--	180,000
			Total	1,307,000

Failure: No internal electrical failure. Delamination of dielectric covering on one side led to corona from exposed foil above 4.0 KV.

*Corrected for charging time constant ≐ 5.7 millisecond

**Oil cooling employed except for first entry

TABLE XI

DYNAMIC TESTS

UNIT M

Capacitance: 0.317 Microfarads

Working Gas: Helium

Test Log:

Repetition Rate (pps)	Charging Potential* (KV)	Continuous Duty Period (Min.)	Total Discharges
100	6.4	90	540,000
1-100	5.0 - 7.5	--	540,000 (approx.)
		Total	1,040,000

Failure: Electrical breakdown occurred in central termination region in vacuum only. Unit has since withstood high potential tests at atmospheric pressure. In this instance cause of failure was attributed to mechanical damage in this region prior to dynamic testing. No delamination was observed.

*Corrected for charging time constant ≐ 4.8 milliseconds

TABLE XII

DYNAMIC TESTS

UNIT N

Capacitance: 0.336 Microfarads

Working Gas: Helium and Argon as indicated

Test Log:

Repetition Rate (pps)	Charging Potential* (KV)	Continuous Duty Period (Min.)	Working Gas	Total** Discharges
1-100	3.0-6.0	--	He	208,361
100	3.5	248	A	500,146
200	2.5		A	528,779
400	1.5		A	2,028,859
1000	0.8		A	2,011,245
2000	0.4		A	231,648
100	3.5	43	A	259,162
10	6.0	9	A	5,280
5-10	3.5-4.0	20	A	64,821
10	6.0	18	A	10,598
10	6.0	50	A	30,019
30	6.0	14	A	25,184
50	5.9	4	A	10,069
10	7.0	40	A	24,081
			Total	5,938,252

Failure: No Failure

*Corrected for charging time constant ≐ 5.1 milliseconds

**Counter readings

TABLE XIII

DYNAMIC TESTS

UNIT O

Capacitance: 0.806 Microfarads

Working Gas: Argon

Test Log:

Repetition Rate (pps)	Charging Potential (KV)*	Continuous Duty Period (Min.)	Total Discharges**
100	2.2	67	101,056
50	3.2		20,436
50	4.0		102,492
50	4.8		25,860
50	4.8	11	30,297
5-10	6.0	--	14,872
5	7.0	12	3,606
		Total	298,619

Failure: No failure

*Corrected for charging time constant ≐ 12 millisecond

**Counter readings

NOTE - This capacitor differs from the nominal ESC-247-C in that it has a capacitance of 0.8 microfarads.

4.3. Thermal Measurements

One facet of the program was that concerned with the thermal characteristics of the capacitor plasma gun system. As noted above, the dynamic system was designed with thermal isolation of gun and capacitor where the gun was mounted by means of an insulating stand-off and a vacuum environment ($< 10^{-4}$mm Hg) was created to eliminate convective heat loss. It was then possible to explore thermal distributions resulting from heat generation under conditions of radiational cooling alone. The system was equipped with the added capability for cooling the terminals of the plasma gun to limit the temperature rise at the connections to the capacitor.

Insight into the distribution of heat sources from dissipated electrical energy may be gained from an analysis of four principal mechanisms: (1) dielectric loss in the capacitor, (2) ohmic heating in the current carrying elements of the system, (3) ohmic losses in contact resistance and (4)heat transfer from the plasma to the acceletator electrodes. Considerations of these heat sources were given in Section 3.1.

In that section an efficiency parameter was defined in Equation 1 in terms of the effective series resistance pertinent to each of these heat sources. Such a parameter does not relate directly to propulsion efficiency. Instead, it is a measure of the total discharged energy which does not eventually appear as heat in the system. The efficiency parameter, therefore, does not distinguish between radiation, internal plasma energy and directed kinetic energy as mechanisms for power output.

Estimates of η based on measurements described below suggest values of approximately 0.30. Then the total fraction of stored energy (or average power) going into thermal energy is about 0.70. In this case the heat produced in the plasma gun is believed to exceed that generated within the capacitor by at least a factor of six. The gun, therefore, constitutes a substantial heat input to the capacitor which can seriously upset the temperature uniformity assumed in the computation of Figure 4 as demonstrated below. A substantial thermal gradient is created near the terminals of the ESC-247-C owing to this heat input and the thermal diffusion characteristics of the capacitor. The result is a temperature rise in the terminal region considerably above that appearing in the outer portions of the capacitor.

Thermal energy produced in the plasma gun is readily transferred to the capacitor terminals whence it is conducted radially outward by means of the foil tabs, the dielectric material and the epoxy build-up at the terminal. A solution of the heat flow equation indicates that conduction in the foil tabs is dominant. The predicted radial temperature gradient at the outer edge of the termination per watt conducted outward (to the radiating surface) is given by:

$$\frac{\Delta \theta}{\Delta R}_{r = 2\text{in.}} = 0.70 \ (^{\circ}\text{K/cm-watt})$$

In contrast to this, the predicted gradient at a radius of 2.5 inches (coinciding with the inner radius of capacitor foils) is only:

$$\frac{\Delta \theta}{\Delta R}_{r = 2.5\text{in.}} = 0.06 \ (^{\circ}\text{K/cm-watt})$$

The predicted gradient then decreases further with increasing radius owing to the increasing cross-section of copper foil material. In obtaining these approximate estimates azimuthal asymmetry in the heat conduction paths have been ignored as well as the thermal coupling across alternate layers of dielectric and foil.

In the evaluation of Units J and K the terminal temperature was monitored continuously. For this purpose a copper-constantan thermocouple was attached to one of the mounting lugs of the terminal. The thermocouple output, referenced to a room temperature junction, was displayed and recorded by means of a chart recorder. The maximum observed temperatures noted in the tabulations of the previous section occurred within approximately 15 minutes indicating that this is typically the time required for thermal equilibrium.

The recorded terminal temperatures are considerably higher than would be expected in the absence of thermal gradients. For example, the average power discharged in the 10 pps operation of Unit K is 30 watts. If all of this power appeared as heat uniformly distributed in the capacitor, the capacitor temperature rise would be expected to be less than 10^{o}C above ambient. The observed terminal temperature rise, however, was approximately 40^{o}C above room temperature and is indicative of the large gradient produced by the heat flux from the plasma gun.

Provision for oil cooling of both plasma gun flanges was made and the thermal gradient was further explored during the evaluation of Unit L. Temperature was monitored at six thermocouple stations located along a radius of the test unit as indicated in Figure 18. Thermocouple #1 was placed at one mounting stud location on the plasma gun flange. The other five thermocouples were bonded to the dielectric surface of the unit as shown. A multiple position switch permitted a scan of the six readings in less than thirty seconds.

Data were recorded for a variety of repetition rates with and without oil cooling. Representative sets of data are illustrated in Figure 19. The set marked (A) was obtained after thermal equilibrium for operation at 10 pps with a charging potential of 4.0 kilovolts. No cooling was used for set (A). Set (B) was taken at equilibrium for 100 pps operation at 3.2 kilovolts with cooling. The temperature rise indicated is relative to room temperature.

In both cases the predicted steep thermal gradient is noted near the capacitor terminals. This confirms not only that heat transfer near the terminals is restricted by the thermal conduction in the foil tabs, but also that the principal source of heat is within the plasma gun as expected.

During the evaluations of Units N and O some initial measurements were made regarding the total heat generated in the capacitor-gun system. Constant flow calorimetry was employed making use of the oil cooling system to measure the extracted heat.

In the constant flow method, one thermocouple immersed in the input flow serves as the reference junction for a second sensor placed in the

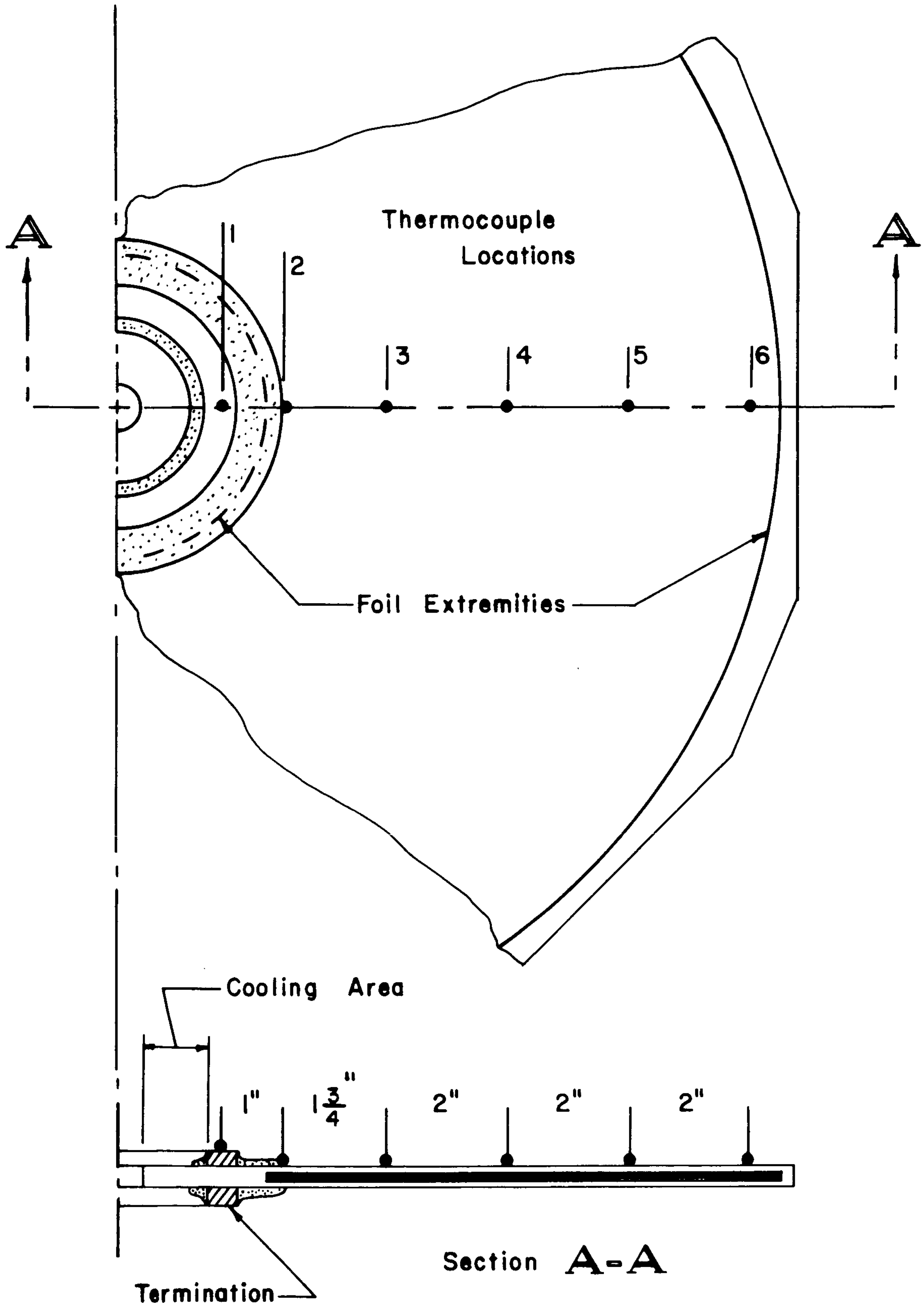

FIGURE 18
THERMOCOUPLE LOCATIONS FOR UNIT L
DYNAMIC OPERATION

21-A1172

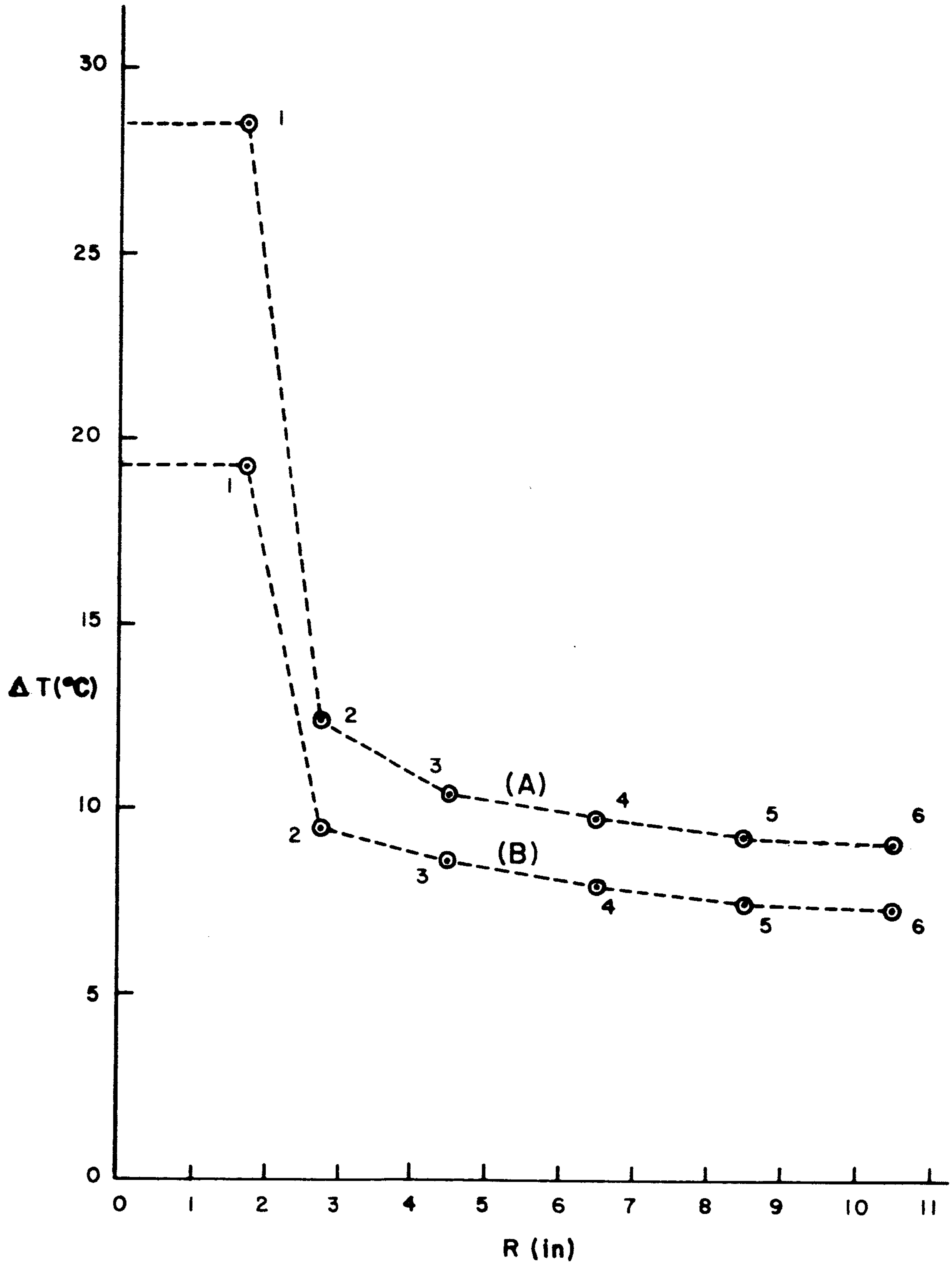

FIGURE 19.

OBSERVED THERMAL GRADIENTS DURING UNIT L DYNAMIC OPERATION

21-A1173

output line. The net signal is then a measure of the temperature difference $\Delta\theta$ between input and output flows. If R is the flow rate in gm/sec, the heat extracted per unit time is given by:

$$P = R \cdot c \cdot \Delta\theta \qquad \text{(watts)}$$

where c is the specific heat of the fluid in joules/gm$^{\circ}$C.

In order to obtain a complete estimate of the fraction of input electrical power converted to heat it is also necessary to consider the radiant heat loss from the capacitor and the heat conduction through supports. It is easy to show that the latter represents less than one per cent of the radiation loss owing to the insulating support employed. This loss can therefore be neglected.

Radiation loss is not known exactly but has been estimated based on the thermal profile data represented in Figure 19. Effectively, an upper bound was computed by assuming an ideal radiator with the appropriate profile. While these profiles were not determined in Unit O and Unit N operation, reliance was placed on scaling the thermal distribution according to the measured flange temperature. Confidence in this approximate procedure was gained from the apparent scaling illustrated in Figure 19. Error in estimating the loss by radiation is thought to be such that an overestimate is made. This leads to an underestimate of the efficiency parameter defined previously which can be written in terms of the measured variables as

$$\eta = \frac{P_i - P_c - P_r}{P_i}$$

where: P_i is the average electrical power discharged by the capacitor, P_c is the power extracted by the oil cooling and P_r is the estimated thermal power radiated by the capacitor. The parameter η then represents the fraction of the electrical input power not ultimately converted to heat within the system consisting of the storage capacitor and the plasma gun.

Measurements of η indicate values in the range of 25 to 35% with some confirmation that η increases as expected with increasing energy stored. The following table presents results obtained during three long period evaluation runs using Units N and O. In each case, the data were taken near the conclusion of the run when thermal equilibrium was assured.

The trend toward higher values of the efficiency parameter for higher energy stored in the capacitor is indicated from these results. Data obtained in two shorter duration operations at storage energies of 4.1 and 9.2 joules per discharge yield estimated efficiency parameters of 31% and 38% respectively. These data, while in accord with the above results, are less reliable since thermal equilibrium was not reached. Nevertheless, the results at each energy storage value are plotted in Figure 20 to illustrate the trend.

4.4. Plasma Gun Performance

The plasma accelerator employed in the dynamic evaluation phase of this program was designed to provide a load representative of a class of pulsed plasma thrusters. The design of the coaxial device used was described above. No attempt was made toward sophisticated design with respect to performance as a thruster, nor were any dynamic measurements made of the plasma acceleration characteristics. On the otherhand, a number of interesting observations were made which are worthy of note as they have a bearing on the special problems of high repetition rate operation.

In regard to obtaining stable high repetition rate operation of the plasma gun, it was necessary to cope with three problem areas. The first of these was concerned with the need to obtain a reliable triggering scheme to control accurately, the discharge pulse rate at any desired value up to 1000 pps. This need was very successfully satisfied by the method described above. A second suspected problem area centered around the possibility of the development of a glow discharge or elongated deionization period which would hinder high pulse rate operation. While this problem did arise, it was traced to a simple geometric cause and was successfully

TABLE XIV

EFFICIENCY PARAMETER MEASUREMENTS

TEST UNIT	UNIT N	UNIT O	UNIT O
Repetition Rate (pps)	100	100	50
P_i, Input Power (watts)	205	201	321
Energy per Discharge (joules)	2.05	2.01	6.45
Total Discharges	5×10^5	1×10^5	1×10^5
ΔT, Oil Flow Temperature Difference (°C)	9.3	9.4	13.0
Flange Temperature	35	35	49
R, Oil Flow Rate (gm/sec)	5.51	5.51	5.51
C, Oil Specific Heat (joules/gm°C)	2.23	2.23	2.23
P_c, Power Extracted (watts)	110	111	154
P_r, Power Radiated (watts)	38	38	52
η, Efficiency Parameter	28%	26%	36%

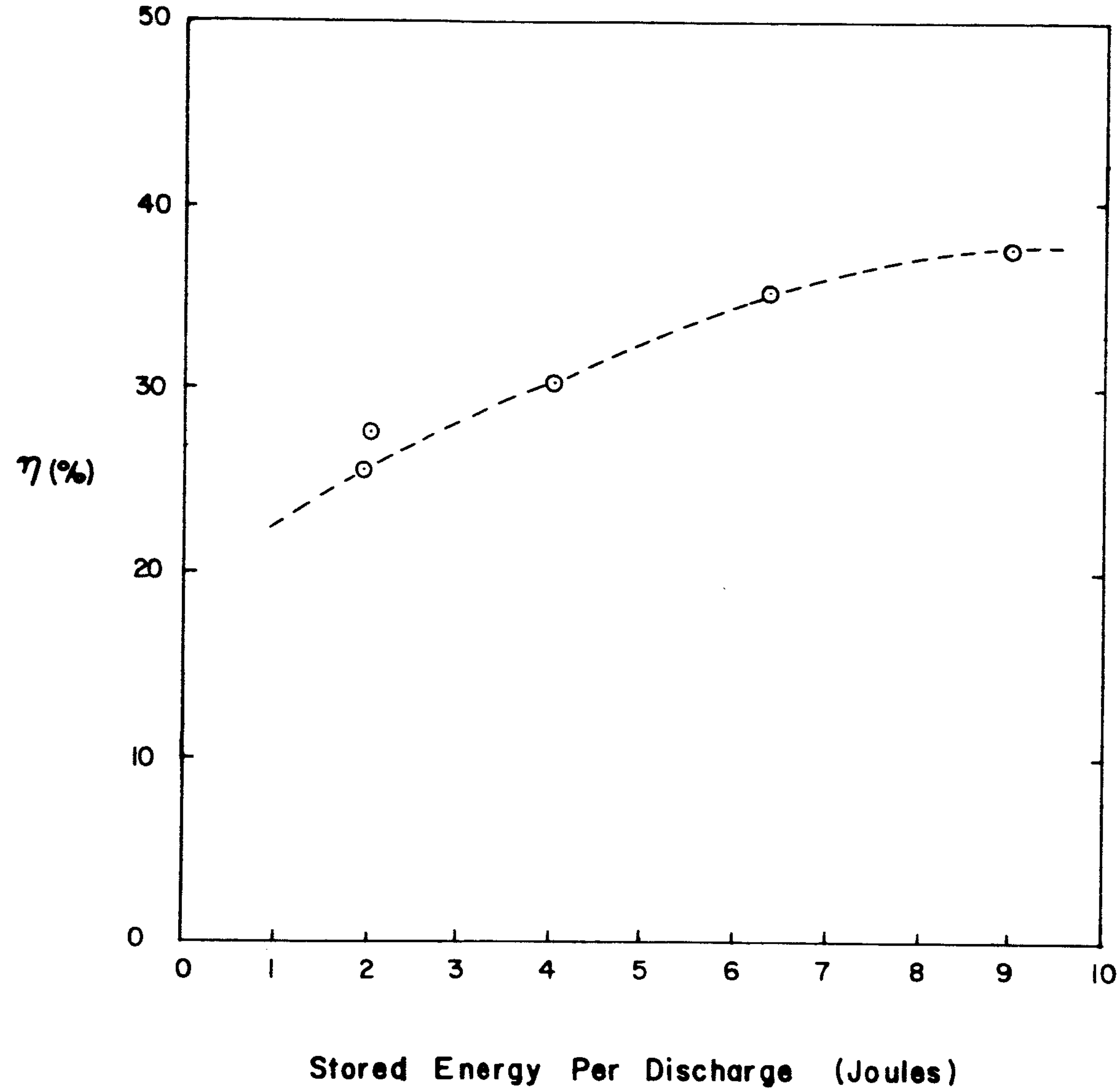

FIGURE 20

EFFICIENCY PARAMETER VARIATION
WITH STORED ENERGY

21-A1174

eliminated. Finally, the problem of power handling capacity arose, not only in regard to heat dissipation, but also in regard to electrode erosion and insulator life. The deterioration rate of insulators exposed to the discharge was unexpectedly high and was a persistent cause of difficulty. The experience in each of these areas is discussed in more detail in the following paragraphs.

The designed function of the triggering system has been described above. In the early stages of the program helium was used as working gas. In order to obtain reliable operation of the trigger, it was necessary to use flow rates such that the gun operated into an ambient of at least 150 microns - Hg. At lower pressures, it was not possible to breakdown the gas within the trigger electrode region. This pressure was such that conditions were very close to those necessary for the development of a glow discharge between the center conductor of the gun and remote ground potential fixtures within the gun enclosure. While a potential of at least 9 KV was held-off between the center conductor of the gun and ground, pulsed discharge operation led to the gradual development of a long-path glow discharge which eventually led to a high current discharge. The latter prevented sustained pulsed operation at pulse rates above about 10 pps. Normally, the gun has been operated with the center conductor initially at high potential negative. Reversal of polarity eliminated the glow problem, but had an adverse effect upon the triggering reliability. The problem was resolved by shortening the center conductor so that electric field lines from the tip of the center conductor were terminated on the inside wall of the outer conductor. Long paths necessary for breakdown at the pressure employed in the gun enclosure were thereby eliminated. With this simple modification, triggered operation in helium was possible at repetition rates exceeding 100 pps. However, the gas pressure in the gun environment was somewhat higher than desired under conditions which were favorable for reliable triggering. While quite stable operation could be maintained for as long as three hours, missfires (failure of the trigger to ignite the discharge) occurred, typically, at the rate of 1 to 10%. In an estimated 50 to 75% of discharges, a spoke discharge was observed predominately in the area of the breech. This was attributed to one of two causes: non-symmetrical initiation of the discharge, or the tendency for a crow-bar discharge to develop within the gun at one or more current reversals. Later experience would suggest that the former cause was most likely. Because of the high dielectric strength of helium at low pressure, trigger pulse voltage was near its maximum value (10 KV) and trigger pulse breakdown was somewhat erratic due to the statistical characteristics of the breakdown process.

In the evaluation of Units N and O, it was found that the use of argon as working gas, removed all of the above difficulties. At gun envelope pressures of 25 microns - Hg, the triggering stability was excellent for pulse voltages as low as 2 KV. Pulse rates of less than 1 pps to 2000 pps (twice the design limit) were readily obtainable without any extensive adjustment of operating parameters. Missfire rate under best conditions was estimated at less than 0.01%. The plasma discharge was perfectly uniform (azimuthally) insofar as qualitative visual observations could distinguish. The discharge spectrum strongly peaked in the ultraviolet as is characteristic of an electrical discharge in argon at low pressure. Spoke-type discharges were notably absent with an estimated rate of occurance of 0.1%. This rate under best conditions was much less, but was noted to increase as the breech insulator deteriorated.

Waveform observations of the light intensity from the plasma discharge were performed by means of the photocell employed in the discharge counting scheme. The light pulse was viewed along the accelerator axis. The frequency response of the photocell circuit was approximately 3 Mc. During operation with argon, the oscilloscope trace was reproducible to the extent that pulse-to-pulse variations were generally indistinguishable. Fluctuations in the light signal were introduced only when there was a missfire (rare) or a spoke discharge.

A typical light pulse for argon operation is nearly exponential with a decay time constant of about 14 microseconds. Assuming that this time is also approximately equal to the decay time of ionization in the discharge, or equivalently to the discharge extinction time, it should be possible to obtain pulse rates as high as 10^4 pps or even slightly higher. Of course, the observed decay rate is dependent upon electron recombination and diffusion processes which are functions of the geometry and the gas pressure. Therefore, the conclusion regarding an upper limit to the pulse repetition rate must be considered in this light. As an experiment in the program, the pulse rate was increased in one case to 2000 pps. It was not practical to attempt higher rates since the trigger pulse was designed for a maximum of 1000 pps operation.

The rise time of the observed light pulse is approximately 2 microseconds. This corresponds to several cycles of the discharge current waveform which was determined to have a ringing frequency of about 2.5 Mc and a Q of approximately 10. Thus, the light intensity rise time corresponds to the current decay time. The light waveforms showed evidence of intensity fluctuations consistent with current oscillation during the overall intensity build-up.

As a basis for the initial design of the plasma gun, a simplified snowplow calculation was made of the acceleration. While no attempt was made in the program to explore the relationship of theory and dynamic measurement of the plasma motion, observations of the eroded electrodes provided an interesting comparison. Following each long term operation of the plasma gun, the center electrode was observed to be eroded for a distance of several centimeters from the region of the trigger holes toward the muzzle of the accelerator. The degree of erosion was noted to decrease gradually along this path so that the exact distance was not determinable. However, within the accuracy possible, the eroded length and the predicted displacement of the plasma (during acceleration) were in remarkable agreement. Moreover, the approximate agreement was seen to exist for the variety of energy storage values employed.

In these cases, the eroded length varied from approximately 3 to 10 cm. The possibility that this agreement is fortuitous is recognized and is pointed up by the fact that erosion of the inner wall of the outer electrode did not match the extent (in downstream length) of that observed for the center gun electrode. Since the axial length of the former was in all cases smaller than noted above, indications are that the discharge current is not exclusively radial throughout the discharge. It is believed that a substantial axial component of discharge current develops during the acceleration phase.

The erosion of electrodes was not a serious problem in the investigation. The outer electrode of the plasma gun was cleaned periodically, but it was not replaced throughout the program. The center electrode (initially at high negative potential) was replaced several times, largely because of the enlargement of the trigger holes. Otherwise, material removal was neglible as regards dimensional changes.

The principal problem involving material damage in the plasma gun was that associated with the breech insulator. In the early stages of dynamic evaluation, organic breech insulation was seen to decompose very rapidly. The experience with several materials and insulator geometries led to the scheme illustrated in the gun design depicted above. Capacitors were prepared for dynamic testing by filling the central through hole region of the unit with an epoxy resin containing a high percentage of alumina powder as a filler. A pyrex sleeve was sealed into the capacitor and alligned to accomodate the central conductor of the plasma gun. The pyrex sleeve provides an elongated path against surface breakdown and ensures that inorganic material only will be near the plasma discharge.

This technique was completely satisfactory for most of the dynamic tests, since the capacitor life was in most cases less than the gun insulator life. In the evaluation of the last two units, Units N and O, the limited insulator life prevented a full life test as the capacitor life exceeded insulator life. The cause of insulator failure was eventually traced to the formation of a corona discharge originating on the outside surface of the pyrex sleeve. This was particularly evident during the stable argon operation of the plasma gun in which small corona spots were observed migrating over the insulator surface. Failures occurred as the corona gradually decomposed the pyrex to the extent that breakdown through the insulator took place. Insulator life decreased rapidly with increased capacitor potential. For example, in Unit N operation, a total of more than 5×10^6 discharges were logged in continuous operation below 3.5 KV, while only 3×10^4 discharges were typically possible with a single insulator when the operating potential was in the range 6 to 7 KV. Higher average power also had the effect of reducing insulator life, but this dependence was secondary.

In summary, the experience obtained points up a problem area regarding insulator decomposition by corona discharge. On the otherhand, the triggering technique has been employed with considerable success and the feasibility of obtaining controlled high repetition rates in the pulsed plasma gun has been demonstrated up to repetition rates of 2000 pps.

5. Summary and Recommendations

5.1. Summary of Results and Conclusions

Analysis carried out early in the program pointed to the need for emphasis in capacitor development on the use of high temperature, low dissipation dielectric materials. Self-generated heat in capacitors designed for high repetition rate duty, coupled with the needs for maximum power-to-weight ratios and radiational cooling leads to operating temperatures far above the capability of conventional capacitors. The fraction of capacitor stored energy dissipated within the capacitor is equal to the ratio of the discharge circuit Q to the Q of the capacitor operating into a lossless load. This fraction typically ranges between 5% and 20%. In achieving a balance between the heat internally generated and the thermal radiation loss, equilibrium temperature in the capacitor must be substantially above ambient. For capacitors evaluated in this program, the operating temperature is predicted to range from $250^{\circ}C$ for capacitors whose $Q = 50$ to about $140^{\circ}C$ for capacitors with $Q = 200$ when operation is at discharge rates of 1000 pps. This example points to the need for low loss, high temperature materials. The high temperature capability is made increasingly important where the capacitor may be called upon to radiate additional thermal inputs, eg. from the plasma accelerator portion of the discharge circuit. Reduction of capacitor dissipation (higher Q) also contributes toward higher ultimate system efficiency.

In view of these needs, the problem which presented itself in the development of a suitable capacitor centered around the selection of a low loss, high temperature dielectric material and the fabrication of a laminated capacitor employing such material. The over-all capacitor construction layout and geometry were adapted and scaled from the available flat disc capacitor design. Capacitors fabricated prior to the program employed Mylar as a dielectric. Initial evaluative testing was performed on fabricated capacitors using this material to provide a basis for comparison with improved dielectrics developed later in the program. Additional plastic films including Teflon and H-Film were evaluated with regard to their general dielectric properties.

On the basis of its high temperature mechanical limits and excellent dielectric properties, Isomica was selected from the available materials as a practical first step toward realizing program goals.

During this program, the many difficulties of laminating large capacitors with Isomica dielectric were overcome. While the full capability of the Isomica capacitor has not been realized, it is clear that a substantial gain has been made.

Successful and partially successful capacitors fabricated with Isomica were subjected to dynamic tests in addition to the usual tests of the quality assurance type following manufacturing cycles. Dynamic testing was conducted with the capacitor discharging repetitively into a coaxial plasma gun as the test load. The capacitor-gun system was thermally isolated in vacuum to enable investigation of the thermal transport properties of the capacitor under conditions of minimal conduction and convection heat loss and to illuminate any problem areas with regard to outgassing or mechanical effects in vacuum. Problems of the latter type, while severe in first units where lamination was not perfected, were not in evidence in the later units evaluated. Thermal data highlighted the problem area of thermal gradients produced by heat input at the capacitor terminations from heat sources in the load.

Capacitor failures occuring in the early phases of dynamic testing were caused by delamination and breakdown of the surface tracking type. Later units were subjected to several million discharges without degradation of the capacitor. At this point capacitor life far exceeded the continuous operating life of the plasma gun used as the test load. During the course of the dynamic testing, no capacitor failures were encountered which could be attributed to electrical puncture of the dielectric material. In this regard, it must be considered that all dynamic evaluation was carried out at stress levels below 1000 volts/mil.

The need in the program to develop means for simulating the load characteristics of pulsed plasma thrustors has led to some important by-products regarding high repetition rate duty. A means has been developed for efficiently triggering a coaxial plasma gun. The method used controls repetition rate accurately at pulse rates to well over 1000 pps. At the same time there is essentially no interference with gun design requirements for low self-inductance and close coupling to the capacitor. The use of a gun with this trigger scheme has demonstrated the feasibility of high pulse rates for plasma acceleration.

5.2. Recommendations and Future Proposed Work

Substantial progress has been made under this program toward the development of very low inductance capacitors with capability for high temperature operation and other desirable properties. Using Isomica as a dielectric it is believed that capacitors can be manufactured which have internal self inductance less than one nanohenry, Q as high as 100 to 200, dielectric strength for average duty above 2000 volts per mil and operating temperature around 200°C. To realize this potential, further development work is required to perfect fully the processing of capacitors using this material.

While Isomica has emerged as a superior dielectric as compared to other materials evaluated in this program, additional survey and evaluation should be accomplished to seek other materials which might have a capability for extending performance still further. This investigation should be concerned with material properties which relate to capacitor fabrication processes as well as the electrical and thermal properties.

The general laminated capacitor concept in the flat disc geometry is well suited to low inductance design with additional advantages in providing good form factor for radiative cooling. The particular form evaluated in this program, however, does not readily allow for extension to energy storage with many electrically parallel elements. Therefore, it is proposed that further work concern itself with geometries which will lend themselves to parallel stacked arrangements of many capacitors.

Measurement of the capacitor performance and thermal behavior should be continued under vacuum conditions and with simulated loads. In the dynamic testing at increased power levels it will be necessary to cope with those problems which limit plasma accelerator life since, at present, capacitor life is such as to exceed the sustained operating period of the plasma gun. A particular problem area is the deterioration of insulating materials which are in contact with the plasma.

Work concerned with the efficiency, sources of heat and thermal transport in capacitor-plasma gun systems should receive considerable attention. This effort will contribute to knowledge of the thermal properties of capacitor and will also provide preliminary insight into the thermal distribution problems to be dealt with eventually in actual space borne pulsed propulsion systems.

DISTRIBUTION

Recipient		Address
RNT/James Lazar RNT/J. Mullin	(1) (1)	NASA Headquarters FOB - 10 B 600 Independence Avenue Northwest Washington, D. C. Attention: RNT/James Lazar RNT/J. Mullin
Patent Counsel	(1)	NASA Lewis Research Center 21000 Brookpark Road Cleveland, Ohio 44135 Attention: Norman T. Musial
J. Howard Childs A. E. Anglin H. G. Kosmahl P. Ramins	(2) (1) (1) (10)	NASA Lewis Research Center Spacecraft Technology Division 21000 Brookpark Road Cleveland, Ohio 44135 Attention: J. Howard Childs A. E. Anglin H. G. Kosmahl P. Ramins
Lewis Library	(2)	NASA Lewis Research Center 21000 Brookpark Road Cleveland, Ohio 44135 Attention: Library
Lewis Technical Information Division	(1)	NASA Lewis Research Center 21000 Brookpark Road Cleveland, Ohio 44135 Attention: Technical Information Division
John H. DeFord	(1)	NASA Lewis Research Center Spacecraft Technology Procurement Section 21000 Broopark Road Cleveland, Ohio 44135 Attention: John H. DeFord
NASA Representative RQT-2448 *Plus a reproducible copy.	(6)*	NASA Scientific and Technical Information Facility Box 5700 Bethesda, Maryland 20014 Attention: NASA Representative/RQT-2448

Recipient		Address
W. Moeckel E. Reshotko G. Seikel D. J. Michels	(1) (1) (1) (1)	NASA Lewis Research Center Electric Propulsion Division 21000 Brookpark Road Cleveland, Ohio 44135 Attention: W. Moeckel E. Reshotko G. Seikel D. J. Michels
P. J. Cannon	(1)	NASA Lewis Research Center Technology Utilization Office 21000 Brookpark Road Cleveland, Ohio 44135 Attention: P. J. Cannon
M. Ellis	(2)	NASA Langley Research Center Langley Station Hampton, Virginia 23365 Attention: M. Ellis
M-RP-DIR/ E. Stuhlinger	(1)	NASA George C. Marshall Space Flight Center Huntsville, Alabama 35812 Attention: M-RP-DIR/E. Stuhlinger
G. Goodwin	(1)	NASA Ames Research Center Moffett Field, California 94035 Attention: G. Goodwin
J. J. Paulson	(1)	Jet Propulsion Laboratory 4800 Oak Grove Drive Pasadena, California 91102 Attention: J. J. Paulson
AFAPL(APIE)/R. Supp		Commander Aeronautical Systems Division Wright-Patterson Air Force Base, Ohio Attention: AFAPL(APIE)/R. Supp
Dr. M. Slawsky	(1)	USAF Headquarters Office of Scientific Research Washington 25, D. C. Attention: Dr. M. Slawsky
T. L. Rosebrock	(1)	Allison Division, GMC Indianapolis, Indiana Attention: T. L. Rosebrock

Recipient		Address
Dr. P. Gloersen	(1)	General Electric Company Space Sciences Laboratory Missile and Space Vehicle Dept. Valley Forge, Pennsylvania Attention: Dr. P. Gloersen
Dr. J. Gooding	(1)	General Dynamics/Astronautics San Diego, California Attention: Dr. J. Gooding
Professor O. K. Mawardi	(1)	Case Institute of Technology 10900 Euclid Avenue Cleveland, Ohio 441106 Attention: Professor O. K. Mawardi
Dr. C. L. Dailey	(1)	Space Technology Laboratory One Space Park Redondo Beach, California Attention: Dr. C. L. Dailey
Dr. T. M. Teem	(1)	Electro-Optical Systems, Inc. 125 North Vinedo Avenue Pasadena, California Attention: Dr. T. M. Teem
Dr. V. Blackman	(1)	Magnetohydrodynamics, Inc. P. O. Box 1815 Newport Beach, California Attention: Dr. V. Blackman
R. Edwards	(1)	General Electric Company Flight Propulsion Lab. Evendale, Ohio Attention: R. Edwards
A. N. Thomas	(1)	The Marquardt Corporation Saticoy Street Van Nuys, California Attention: A. N. Thomas
S. Ridgeway	(1)	General Technology Corporation 3510 Torrance Blvd. Torrance, California Attention: S. Ridgeway

Recipient		Address
Dr. R. G. Meyerand, Jr.	(1)	United Aircraft Corporation Research Department East Hartford, Connecticut Attention: Dr. R.G. Meyerand, Jr.
A. E. Kunen	(1)	Republic Aviation Corporation Plasma Propulsion Laboratory Farmingdale, Long Island, New York Attention: A. E. Kunen
T. T. Reboul	(1)	Radio Corporation of America Astro-Electronics Division Princeton, New Jersey Attention: T. T. Reboul
A. S. Penfold	(1)	Litton Systems, Incorporated Beverly Hills, California Attention: A. S. Penfold
Dr. S. R. Byron	(1)	Ford Motor Company Aeronutronics Newport Beach, California Attention: Dr. S. R. Byron
Dr. A.R. Kantrowitz	(1)	AVCO Everett Research Laboratory Everett, Massachusetts Attention: Dr. A. R. Kantrowitz
Dr. H. Mirels	(2)	Aerospace P. O. Box 95085 Los Angeles, California 90045 Attention: Dr. H. Mirels
Dr. E. H. Holt	(1)	Rensselaer Polytechnic Institute Troy, New York Attention: Dr. E. H. Holt
T. K. Kerrebrock & E. E. Covert	(1)	Massachusetts Institute of Technology Naval Supersonic Laboratory Cambridge, Massachusetts Attention: T.K. Kerrebrock & E.E. Covert
Prof. E. L. Resler, Jr.	(1)	Graduate School of Aeronautical Engineering Cornell University Ithaca, New York Attention: Professor E. L. Resler, Jr.

Recipient		Address
D. Bershader	(1)	Lockheed Missile Systems Division Palo Alto, California Attention: D. Bershader
M. E. Maes	(1)	Rocket Research Corporation 233 South Holden Street Seattle, Washington 98108 Attention: M. E. Maes
S. Naiditch	(1)	Unified Science Associates, Inc. 826 South Arroyo Parkway Pasadena, California Attention: S. Naiditch
M. L. Ghai	(1)	Space Dynamics Corporation 2215 Florence Avenue Cincinnati, Ohio 45206 Attention: M. L. Ghai
Dr. R. H. Boden	(1)	Rocketdyne 6633 Canoga Avenue Canoga Park, California Attention: Dr. R. H. Boden
R. T. Craig	(1)	TAPCO Division of Thompson Ramo Wooldridge, Inc. 7209 Platt Avenue Cleveland, Ohio 44104 Attention: R. T. Craig
L. H. Kroger	(1)	Ion Physics Corporation P. O. Box 98 Burlington, Massachusetts Attention: L. H. Kroger
Robert H. Postal	(1)	Thomas A. Edison Research Laboratory Division of McGraw-Edison Company West Orange, New Jersey Attention: Robert H. Postal
Library Technical Documents Group	(1)	Aerospace Corporation P. O. Box 95085 Los Angeles, California 90045 Attention: Library Technical Documents Group
Dr. R. Lorbert	(1)	General Atomic/General Dynamics San Diego, California Attention: Dr. R. Lorbert

N65-32958

ERRATA

NASA CONTRACTOR REPORT CR-54087

EVALUATION OF CAPACITORS FOR SPACE

PROPULSION APPLICATIONS

by E. Blank, J. Proud, and A. Winston

Tobe Deutschmann Laboratories

The subject report was incorrectly numbered as NASA CR-54057. Please change this number to NASA CR-54087 on the cover and title page.

TLC correction 2/10/66